3GPP Standardized 5G Channel Model for IIoT Scenarios: A Survey

Article *in* IEEE Internet of Things Journal · January 2021

DOI: 10.1109/JIOT.2020.3048992

CITATIONS
115

READS
2,388

10 authors, including:

Tao Jiang
China Mobile Research Institute
37 PUBLICATIONS **468** CITATIONS
SEE PROFILE

Jianhua Zhang
Beijing University of Posts and Telecommunications
387 PUBLICATIONS **6,973** CITATIONS
SEE PROFILE

Pan Tang
Beijing University of Posts and Telecommunications
77 PUBLICATIONS **1,377** CITATIONS
SEE PROFILE

Lei Tian
Beijing University of Posts and Telecommunications
98 PUBLICATIONS **1,110** CITATIONS
SEE PROFILE

This article has been accepted for publication in a future issue of this journal, but has not been fully edited. Content may change prior to final publication. Citation information: DOI 10.1109/JIOT.2020.3048992, IEEE Internet of Things Journal

3GPP Standardized 5G Channel Model for IIoT Scenarios: A Survey

Tao Jiang, *Student Member, IEEE*, Jianhua Zhang, *Senior Member, IEEE*, Pan Tang, *Student Member, IEEE*, Lei Tian, *Member, IEEE*, Yi Zheng, Jianwu Dou, Henrik Asplund, Leszek Raschkowski, Raffaele D'Errico, *Senior Member, IEEE*, Tommi Jämsä, *Member, IEEE*

***Abstract*—Industrial internet of things (IIoT) is an emerging area that fifth-generation (5G) mobile communication system penetrates industrial manufacturing applications. The indoor factory has larger space and there are a lot of metal machine tools distributed in it, which makes its radio propagation characteristics and corresponding channel models significantly different from those of the indoor office and indoor hotspot. To support the design and the evaluation of the IIoT techniques, the 3rd Generation Partnership Project (3GPP) released the first 5G IIoT standard model in October 2019. In this paper, we give a detailed explanation of this IIoT model and compare it with other indoor models. Firstly, we introduce the standardization of 3GPP IIoT channel model and its motivation. Secondly, four IIoT sub-scenarios, which are classified according to the clutter density and antenna height, are described. Thirdly, the potential frequency bands of 5G IIoT are summarized. Fourthly, the models of channel parameters, including the path loss and the line-of-sight (LOS) probability, the Root Mean Square (RMS) delay spread, and the angular spread, are given. Among them, the models of path loss and LOS probability take the antenna height and clutter density into consideration. The model of RMS delay spread changes from frequency-dependent to volume-dependent in order to catch the size variation of factories. Finally, two newly added key channel characteristics, dual mobility and absolute time of arrival, which help to describe the robot movement and positioning, are also presented.**

***Index Terms*—IIoT, 3GPP, channel model, path loss, LOS probability, RMS delay spread, angular spread**

I. Introduction

INTERNATIONAL Telecommunication Union (ITU) defines three usage scenarios for fifth-generation (5G), namely Enhanced Mobile Broadband (eMBB), Ultra-reliable and low latency communications (URLLC)*, and Massive machine type communications (mMTC). With the commercialization of 5G in 2018 worldwide, the eMBB scenario, which is the human-centric use case for accessing multi-media content, services and data, has been widely used. However, the revenues of this traditional consumer-oriented service are expected to remain close to stagnant at an annual growth rate of 0.75 percent through to 2030 [1]. The mobile communication service providers have to explore new businesses to increase service value. At the same time, the industry urgently needs to build the industrial internet of things (IIoT) wireless network to connect the machines, people, and data. This requirement is consistent with the other two 5G usage scenarios: URLLC and mMTC. According to the report from IHS Markit [2], the global economic output in 2035 enabled by 5G in IIoT usage scenarios, such as manufacturing, transport, construction, utilities, and mining will reach $5 trillion. Among them, manufacturing leads all industries with $3.4 trillion.

Traditionally, the manufacturing industry has been relying on its own solutions, or those retrofitted from the Institute of Electrical and Electronic Engineers (IEEE) family of wireless technologies to support limited connectivity inside factories, plants and warehouses [3]–[5]. With 5G all of these are changing rapidly. A typical hybrid scenario of 5G and IIoT is shown in Fig. 1. Various machines construct an ultra-dense network, which provides a connection density of 1 million devices per square kilometer for IIoT scenarios [6]–[8]. With the help of device-to-device (D2D) communication and mobile/multi-access edge computing (MEC), the end-to-end latency decrease to one millisecond. The reliability of real-time applications, such as automatic guided vehicles (AGVs), remote control mechanical arms, and online computing, increases dramatically. The massive Multiple-Input Multiple-Output (MIMO) and beamforming technologies can cover the devices with different heights and expand the channel capacity of the whole communication system. Furthermore, as the center frequency rises to millimeter wave bands, there will be more available spectrum resources in IIoT.

However, the environment with a large number of machines complicates the radio condition of the factory. The smooth metallic surface creates many reflections, and the considerable body prevents the signal from propagating directly. Even worse, the production process may generate random elec-

T. Jiang, J. Zhang, P. Tang, L. Tian are with the State Key Laboratory of Networking and Switching Technology, Beijing University of Posts and Telecommunications, Beijing 100876, China (e-mail: jet@bupt.edu.cn; jhzhang@bupt.edu.cn; tangpan27@bupt.edu.cn; tianlbupt@bupt.edu.cn).

Y. Zheng is with China Mobile Research Institute, Beijing, China (e-mail:zhengyi@chinamobile.com).

J. Dou is with Algorithm Department, ZTE Corp. Ltd, Shenzhen 518005, China, and with State Key Laboratory of Mobile Network and Multimedia Technology, Shenzhen 518005, China (e-mail: dou.jianwu@zte.com.cn).

H. Asplund is with Ericsson Research, Ericsson AB, Stockholm, Sweden. (e-mail: henrik.asplund@ericsson.com).

L. Raschkowski is with Fraunhofer Institute for Telecommunications, Heinrich Hertz Institute, Berlin, Germany (e-mail: leszek.raschkowski@hhi.fraunhofer.de).

R. D'Errico is with CEA-LETI, 17 rue des Martyrs, 38054 Grenoble, France, and with University of Grenoble-Alpes, 621 Avenue Centrale, 38400 Saint-Martin-d'Hères, France (e-mail: raffaele.derrico@cea.fr).

Tommi Jämsä is with Huawei Munich Research Center, Riesstrasse 25 C3, 80992 Munich, Germany (e-mail: tommi.jamsa@huawei.com).

Manuscript received April 19, 2005; revised August 26, 2015.

*The definitions of used abbreviations in this paper are listed in Table VI in the appendix.

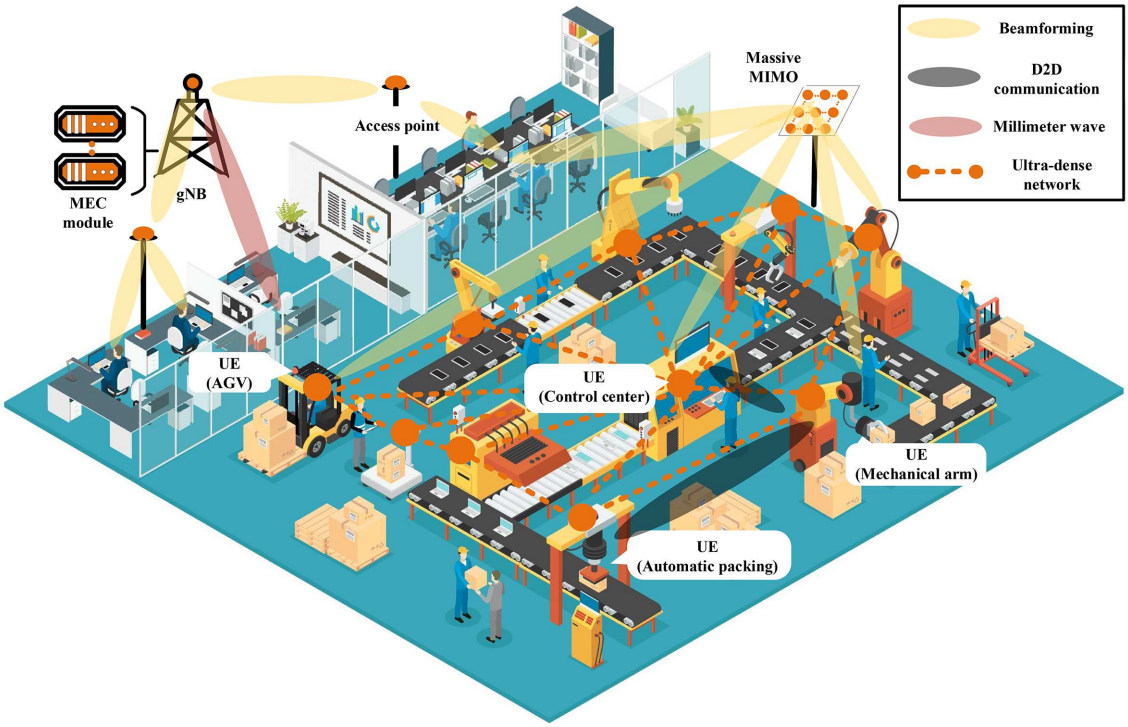

Fig. 1. A hybrid scenario of 5G and IIoT.

tromagnetic noise and interfere with the desired signal. The huge environmental differences make the current standardized indoor channel model unable to be applied to IIoT scenarios. Therefore, it is necessary to study the signal propagation characteristics and to model the wireless channel before designing an efficient and reliable system in such an environment.

A. Related work

The channel modelling research for industrial scenarios roughly experiences three periods. The first period is around 1990. The Digital European Cordless Telephone (DECT) 802.4L and the IEEE 802.11 standards were building wireless communication systems for indoor scenarios [9]. Because this system can effectively reduce the complexity of the connection between machines, it aroused the researchers' interest in indoor factory (InF) scenarios. The narrow-band models were established for the path loss [10] and shadow fading [11]. The wide-band models about delay and multipath were established in [9], [12]. Its path resolution was 7.8 ns and the measured frequency was around 1.3 GHz, which was seen as a good fit to the cellular systems at that time.

The second period is around 2004. IEEE 802.15.4a [13] releases the first standard channel model for Wireless Personal Area Network (WPAN), and the InF is one of its applicable scenarios. This model aims to support a sensor network that has energy-efficient data communication and a low data rate. The studied frequency bands include three parts: around 1 MHz, 100 to 1000 MHz, and 2 to 10 GHz. The most significant difference of this model is that it adopts the Saleh-Valenzuela (S-V) model of ultra-wideband (UWB) communication. More than 500 MHz measurement bandwidth helps to model the power delay profiles intensively. Multipath and cluster power attenuation factors and arrival rates are introduced into channel model as new parameters [14]–[20].

The third period begins in the 3rd Generation Partnership Project (3GPP) release 15, which may also be seen as the first phase of 5G standardization. The channel modelling for InF has become attractive again due to the integration of 5G technologies and the industry 4.0 [21]–[24]. The current 5G channel models mainly include the ITU-R [25], 3GPP TR 38.901 [26], COST 2100 [27], METIS [28], mmMAGIC [29], NYU wireless channel model [30], and QuaDRiGa [31]. They all belong to the geometry-based stochastic channel model (GSCM) family. Compared with the narrow-band model and the UWB model, these 5G models not only extend their application frequency bands to 100 GHz but also add the three-dimension angular information in them [32]–[34]. More importantly, they are applicable to a wider range of scenarios, such as Urban Macro (UMa), Urban Micro (UMi), Rural Macro (RMa), indoor hotspot (InH), indoor office, etc. Channel characteristics of different scenarios can be easily compared in the same model.

A lot of literature has been published on the measurement and modelling for InF wireless channel (overview e.g. in [7]) but none of them has gained widespread acceptance for system design and testing purposes. Considering the unique scene deployment of InF and the request from the industry forum 5G Alliance for Connected Industries and Automation (5G-ACIA), 3GPP approved a new study item on developing a wireless channel model for IIoT. This IIoT model is a part of 3GPP TR 38.901 V16.0.0 standard channel model [35] and it was released in 2019.

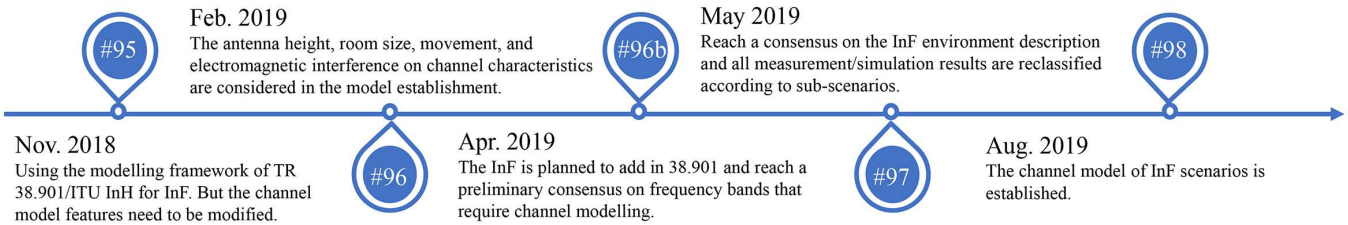

Fig. 2. The reached consensus for InF channel model at meetings.

B. Our contribution

In this article, a comprehensive review of the 3GPP standardized 5G IIoT channel model is conducted. Different from the previous review articles [36]–[38], we not only summarize the existing literature results but also introduce the evolution process of the model from the candidate model to the final model following the process of model standardization. A large number of 3GPP proposals are included here. This review could serve as a reference for 3GPP TR 38.901 standard and also as a fundamental accessory for future studies. To the best of the authors' knowledge, no such article introduces the standardization of this model and its variations at present. The main contributions of this article are as follows:

- Firstly, we introduce the background information about this 5G IIoT channel model released by 3GPP, including the motivation of modelling, the standardization work in the 3GPP, and the evolution process about the standard channel model.
- Secondly, we summarize the environmental characteristics of IIoT scenarios and the frequency bands that have a higher priority in 5G IIoT applications.
- Thirdly, we give a comprehensive introduction about this IIoT channel model:
  - The models of path loss, LOS probability, Root Mean Square (RMS) delay spread, RMS angular spread, absolute time of arrival, and dual mobility are analyzed.
  - The candidate models of path loss, LOS probability, RMS delay spread, and absolute time of arrival are introduced.
  - The model differences, including the applicable scenarios, path loss, RMS delay spread, and RMS angular spread are compared between the InF and indoor office scenarios.

The organization of this article is as follows: the 3GPP standardization process of the IIoT channel model is presented in Section II. Section III introduces the environmental characteristics of IIoT scenarios and Section IV summarizes the potential frequency bands of 5G IIoT. The 5G IIoT channel model is mainly presented in Section V. Three additionally changes in IIoT model are briefly mentioned in Section VI. The conclusion is given in Section VII.

II. Standardization of IIoT channel model in 3GPP

To meet the request from the industry forum 5G-ACIA, the 3GPP Technical Specification Group (TSG) of Radio Access Network (RAN) approved a new study item for the development of an IIoT channel model in meeting RAN #81 [39]. The work was conducted by RAN working group 1 (RAN1) that is responsible for the specification of the physical layer within RAN. This proposal aims to develop a channel model to support studies on URLLC and IIoT enhancements for industrial scenario and use cases. The detailed discussions on this channel model started at RAN1 #95 meeting and ended at RAN1 #98 meeting. Some important reached consensuses of these meetings are presented in Fig. 2 [40]. The different participants, including the industry and academia, contribute data from measurements or simulations [41] to a common pool (path loss, LOS probability, additional delay, etc.), and model parameters are established based on fitting towards this set of data.

After five formal meetings, one informal meeting and several offline discussions, the channel model for InF was established and it was added in the 3GPP TR 38.901 V16.0.0 standard wireless channel [35]. Compared with the former V15.0.0 version [26], the new version has the following changes [42]:

- Added scenario description about InF.
- Added path loss model for InF.
- Added LOS probability model for InF.
- Added two fast fading parameter tables for InF.
- Modified procedure A of spatially-consistent mobility modelling. The BS mobility is also considered.
- Added blocker parameters of automatic guided vehicles (AGV) and industrial robot in blockage model B.
- Added absolute time of arrival model.
- Added dual mobility model.
- Gave simulation methods for electromagnetic interference and embedded devices.
- Added calibration parameters of InF.
- Extended Map-based hybrid model to support InF.

The latest version of 3GPP TR 38.901 is V16.1.0 [43]. This version adds some supplementary notes, but does not modify the models in V16.0.0 version [44]. For the convenience of expression, the 3GPP TR 38.901 standard mentioned below refers to the V16.1.0 version if no individual declaration is made.

III. Environmental Characteristics of IIoT scenarios

The propagation environment is the key factor affecting the wireless channel. Therefore, giving a detailed description of

the target scenario is always the first step when modelling the wireless channel. The typical InF environments include warehouse [45], manufacturing factory [46], automobile factory [23], assembly room [17], etc. They have distinct environment deployment from other indoor scenarios. Compared with the indoor office, which is the only indoor scenario in previous 3GPP TR 38.901, the InF environment has the following features:

- Larger physical size.
- Higher ceiling.
- More metallic objects that produce the specular reflection.
- The objects in the environment have irregular sizes.
- The link blockage is mainly caused by machines rather than walls.

The layout of the indoor office is shown in Fig. 3, and the initially proposed layout of the InF is shown in Fig. 4. From the comparison between them, we can find that the length and width of InF are both larger than the indoor office, which brings InF an additional area of 8400 m^2. To reflect the characteristics of different factories in the same scenario, this InF layout is divided into different functional areas, such as the production area, assembly line, storage/ware house, commission area, and office. But this multi-functional layout of InF complicates the channel modelling. And the limitation of physical size makes the layout rigid. To make the IIoT model applicable in more kinds of industrial scenarios, the physical size of the InF is further defined by the area instead of the length and width. The area of InF scenarios is from 20 to 160000 m^2. When calibrating the accuracy of the IIoT model, we usually choose the scenarios of two sizes, 120×60 m and 300×150 m, as representatives. Besides, the ceiling height of the indoor office is only set to 3 m according to 3GPP TR 38.901. But in the InF, the ceiling height varies from 5 to 25 m. Therefore, the BS antenna can be set to different heights to meet the coverage requirements.

Another difference between the InF and the indoor office is the objects in the environment. The main objects in the indoor office are people, tables, and chairs. Their heights are limited; hence it is appropriate to set the UT height to 1 m, and its nonline-of-sight (NLOS) case is mainly caused by the internal walls. However, in InF scenarios, the objects in the environment are metallic machines. Their huge bodies become the leading blockers in the NLOS case. Because the machine height changes according to their types, varying from 0 to 10 m, it is hard for specifying a fixed value for UT height. To solve this problem, 3GPP TR 38.901 uses "clutter-embedded" and "clutter-elevated" to describe the height of UT and BS. As shown in Fig. 5, the antennas of BS and UT are both clutter-elevated, which means the antenna is higher than the average height of machines. And to make the channel model more practical, the clutter density defined by the clutter-occupied area ratio is also considered. The clutter density is classified into two types, sparse clutter and dense clutter. It's commonly believed that 50% is a dense density. Some other alternative ratio values are proposed in [47], [48]. After the discussions between the 3GPP members, the conclusion is using 40% to classify the sparse or dense density. Considering the effect of

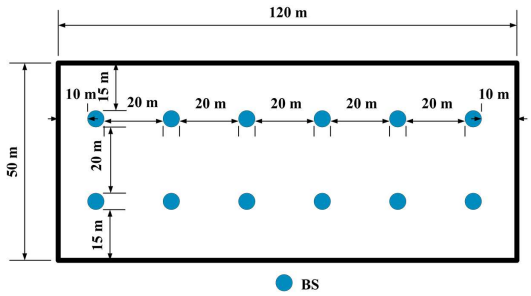

Fig. 3. Indoor office layout [43].

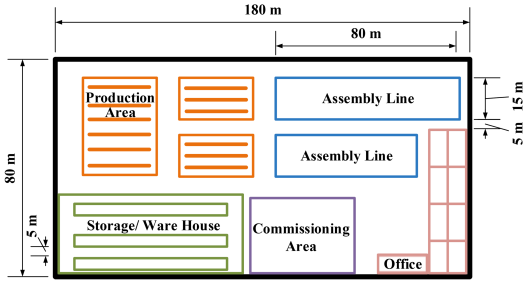

Fig. 4. Proposed IIoT layout by 5G-ACIA [49].

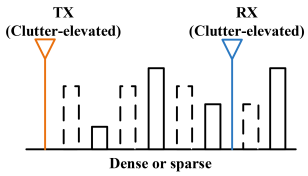

Fig. 5. Sub-scenario in LOS case. The dense environment includes the clutter in dashed line. The sparse environment excludes the clutter in dashed line.

the antenna height of BS and the clutter density, the NLOS cases are divided into four sub-scenarios as shown in Fig. 6:

- Sparse clutter, low BS (SL).
- Dense clutter, low BS (DL).
- Sparse clutter, high BS (SH).
- Dense clutter, high BS (DH).

In the channel calibration part, the setting parameters of InF scenarios are shown in Table I. These settings are more specific and they can be used directly in the system simulation and evaluation.

IV. Potential Frequency Bands of 5G IIoT

The potential frequency bands of 5G IIoT must consider both the existing IoT frequency bands and the 5G frequency bands simultaneously.

The operation frequency bands of IoT sensors mainly have two categories: unlicensed bands and licensed bands. The unlicensed bands are also referred to as the industrial, scientific and medical (ISM) bands. They can be freely used when the radio power is small enough (commonly smaller than 1 w). The typical IoT technologies used in these bands include Bluetooth (2.4 GHz), ZigBee (868 MHz, 915 MHz, 2.4 GHz), WiFi (900 MHz, 2.4 GHz, 5 GHz), LoRa (sub 1 GHz), Sigfox (sub 1 GHz), etc. Although the ISM bands have already been

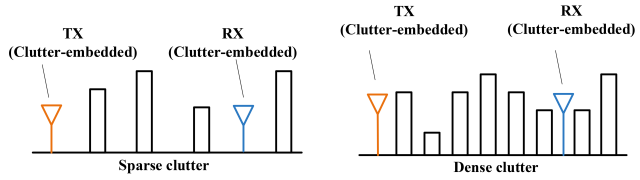

(a) Sparse clutter, low BS (SL). (b) Dense clutter, low BS (DL).

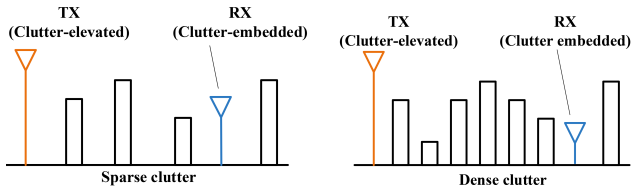

(c) Sparse clutter, high BS (SH). (d) Dense clutter, high BS (DH).

Fig. 6. Four sub-scenarios in NLOS cases.

TABLE I
CALIBRATION PARAMETERS OF LAYOUT [43].

Parameter	Values
Scenario	InF-SL, InF-DL, InF-SH, InF-DH.
Hall size	InF-SL (small hall): 120×60 m; InF-DL (big hall): 300×150 m; InF-SH (big hall): 300×150 m; InF-DL (small hall): 120×60 m.
Room height	10 m
BS antenna configurations	1 element (vertically polarized), Isotropic antenna gain pattern.
UT antenna configurations	1 element (vertically polarized), Isotropic antenna gain pattern.
BS deployment	18 BSs on a square lattice distribute as Fig. 7. For the small hall: D=20 m; For the big hall: D=50 m; BS height=1.5 m for InF-SL and InF-DL; BS height=8 m for InF-SH and InF-DH.
UT distribution	Uniform dropping for indoor with minimum $2D$ distance of 1 m. UT height=1.5 m.
Clutter density	Low clutter density: 20%; High clutter density: 60%.
Clutter height	Low clutter density: 2 m; High clutter density: 6 m.
Clutter size	Low clutter density: 10 m; High clutter density: 2 m.

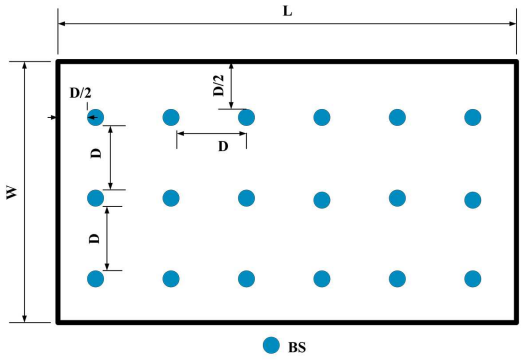

Fig. 7. BS deployment in calibration [43].

designed to 244 GHz [50], the center frequencies of the most research are below 6 GHz [17], [51], [52]. The typical IoT technologies used in licensed bands include NB-IoT (sub 2 GHz), LTE-M (sub 2.7 GHz), etc. These technologies are mainly based on the 3G or 4G licensed cellular network to make data exchange.

With the global commercial use of 5G, the 5G licensed bands, such as 2.6 GHz, 3.4-3.8 GHz, 4.9 GHz, and 28 GHz, are also expected to be applied in IoT scenarios [53]. Among them, the bands 3.4-3.8 GHz are preferred by 5G-ACIA [49]. Besides, the newly identified three frequency bands 24.25-27.5 GHz, 37-43.5 GHz, and 66-71 GHz on World Radiocommunication Conference 2019 will also become the candidate bands for IoT application. Among them, the bands 24.25-27.5 GHz and the bands above 52.6 GHz have higher priority [54], [55]. To enable the smooth application of IIoT technologies in above bands, this IIoT model is developed to support a large range of frequency bands from 0.5 to 100 GHz.

V. THE IIOT CHANNEL MODEL RELEASED BY 3GPP

The 3GPP TR 38.901 channel model is a 5G standard channel model. The generation process of the channel coefficients is illustrated as the flowchart in Fig. 8(a). The whole process is divided into three categories with a total of thirteen modules. In each module, the channel parameters, such as path loss, delay spread, angular spread, and so on, are generated according to the defined models. Although the IIoT scenarios share the same channel coefficient generation process with other scenarios (RMa, UMa, UMi, indoor office, InH), their defined parameter models in the modules are different. The seven most distinct models are highlighted with circled numbers in Fig. 8(a); The evolution process of these models from the candidate models to the final ones as discussed in this paper is illustrated in Fig. 8(b). The numbers in the round brackets are the equation index of this paper.

A. Path loss

There are two widely used path loss models in 5G system. The first one is the alpha-beta-gamma (ABG) model:

$$\begin{aligned}\mathrm{PL}^{\mathrm{ABG}}(f_c, d_{3\mathrm{D}}) = 10\alpha\log_{10}\left(\frac{d_{3\mathrm{D}}}{d_0}\right)+\beta \\ +10\gamma\log_{10}(\frac{f_c}{f_0})+X_\sigma^{\mathrm{ABG}}\end{aligned} \tag{1}$$

where α is the distance-dependent exponent, β is the intercept, and γ is the frequency-dependent exponent. The variable X_σ^{ABG} is the shadow fading which follows a normal distribution with zero mean value. Its standard deviation is denoted by σ. When the measurement results only concentrate on a certain frequency, the ABG model will degenerate into the floating-intercept (FI) model:

$$\mathrm{PL}^{\mathrm{FI}}(d_{3\mathrm{D}}) = \beta^{\mathrm{FI}} + 10\alpha\log_{10}\left(\frac{d_{3\mathrm{D}}}{d_0}\right) + X_\sigma^{\mathrm{FI}} \tag{2}$$

The β^{FI} is the substitute for the frequency-dependent and the β parts in the ABG model, and it is derived from data fitting.

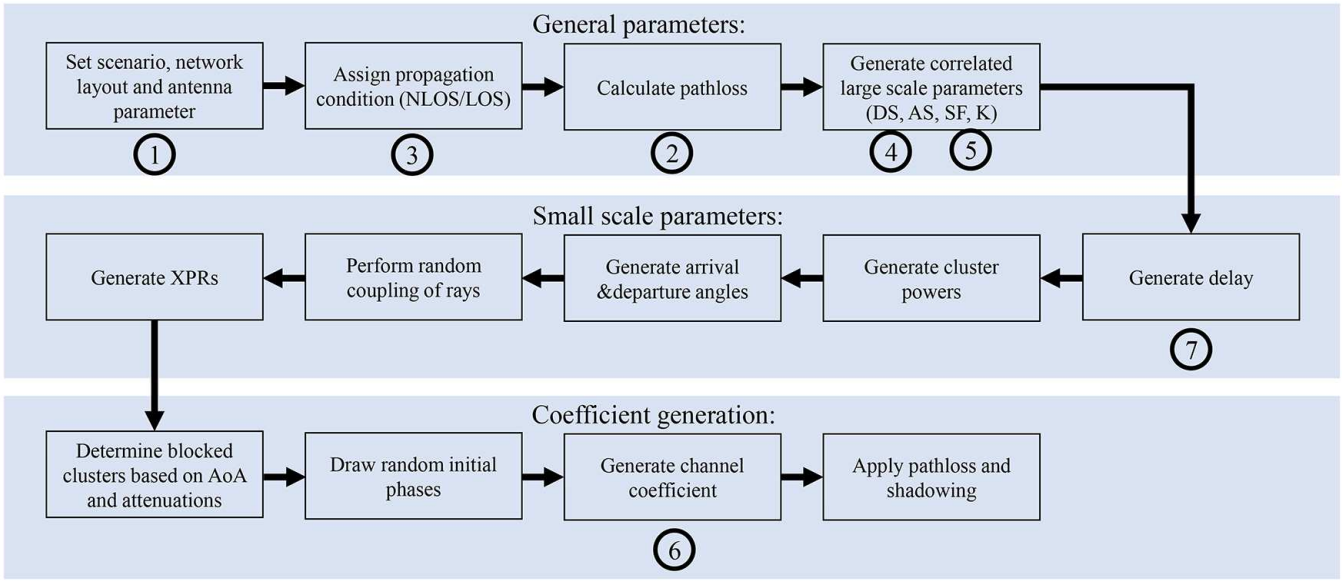

(a) The flowchart of the model coeficient generation in 3GPP TR 38.901 standard [43].

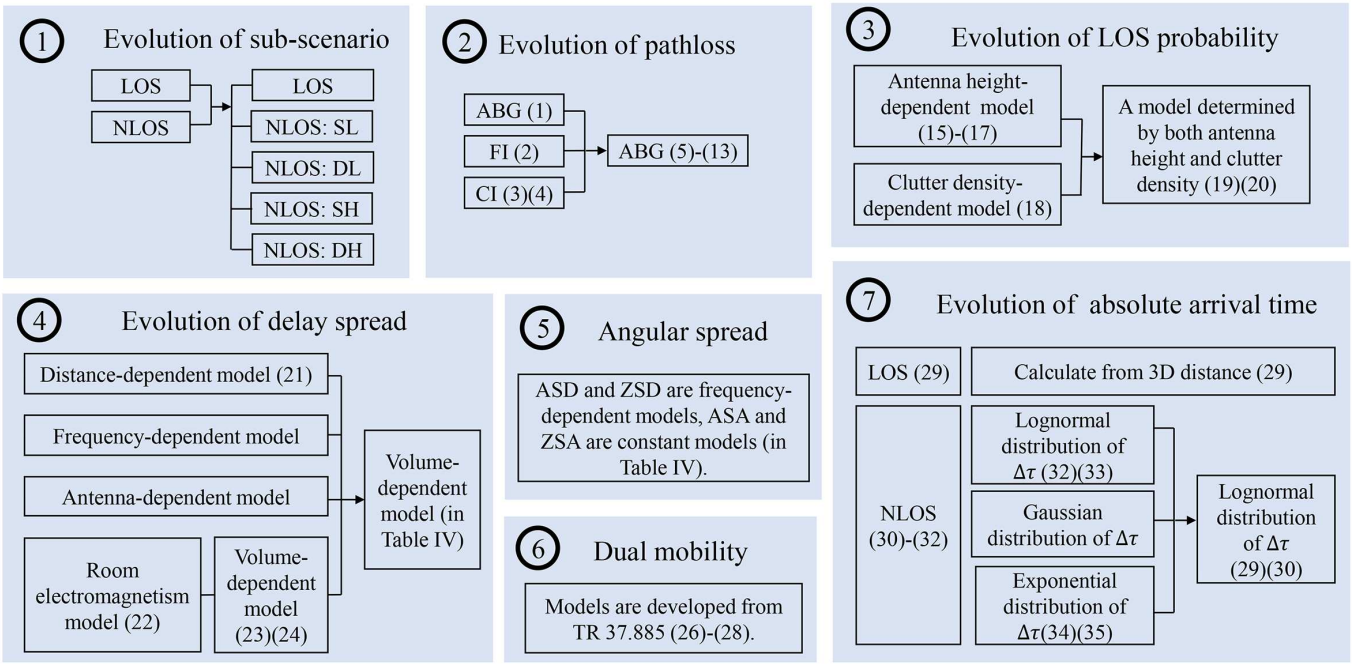

(b) The evolution chain of different IIoT channel parameters. Note: the numbers in the round brackets are the equation index in this paper.

Fig. 8. IIoT channel coefficient generation procedure in 3GPP TR 38.901 standard.

The second one is the close-in free space (CI) path loss model:

$$\mathrm{PL}^{\mathrm{CI}}\left(f_c, d_{3\mathrm{D}}\right) = \mathrm{PL}^{\mathrm{CI}}\left(f_c, d_0\right) + 10n\log_{10}\left(\frac{d_{3\mathrm{D}}}{d_0}\right) + X_\sigma^{\mathrm{CI}} \tag{3}$$

where n is the distance-dependent exponent, f_c is the center frequency, and X_σ^{CI} denotes the shadow fading following a normal distribution with standard deviation of σ. The intercept of CI model is calculated from the free space path loss at reference distance d_0 as:

$$\mathrm{PL}^{\mathrm{CI}}(f_c, d_0) = 20\log_{10}\left(\frac{4\pi f_c d_0}{c}\right) \tag{4}$$

The parameter c is the speed of light and equals to $3\cdot10^8$ m/s.

Comparing with the CI model, the parameters α, β and γ in the ABG model are obtained from least square [56] or minimum mean square error (MMSE) [57] fitting. Therefore, the ABG model is closer to the actual measurement results, and it is used in most standard models, such as ITU-R, 3GPP TR 38.901, mmMAGIC, QuaDRiGa, etc. The CI model is proposed in [58] and adopted as the indoor path loss model

in the ITU-R and 3GPP TR 38.901. It physically chooses the free space loss at 1 m as the intercept, and its exponent n is the best fit MMSE over all measurements. When modelling the path loss for InF scenarios, both models are candidates. To avoid over-fitting the parameters of the ABG model in NLOS cases, the 3GPP model additionally uses the free space loss or the LOS path loss as a minimum [47], [59].

In addition to determining the kind of path loss model, we also need an accurate modelling method for different types of factories. A suitable method is to divide them into different sub-scenarios. As shown in Table II, the clutter density affects the path loss a lot. Especially in NLOS cases, the exponent n increases from 2.53 to 4.38 and the shadow fading standard deviation (std) σ increases from 5.71 to 8 dB when the clutter density changes from sparse to dense. Besides, the path loss is also sensitive to the antenna height in the NLOS case [60]. In [61], the path loss has 4 to 5 dB variance when the antenna changes from embedded to elevated. In [62], the path loss exponents in the CI model prove to decrease with increasing BS height. They are approximately 2.5 in the clutter-elevated sub-scenario and 3.2 in the clutter-embedded sub-scenario. Through the above observations, we can find that the path loss of InF is mainly affected by the clutter density and the antenna height. Especially in the cases of NLOS, this effect is particularly prominent. Therefore, the NLOS cases of the InF are divided into four sub-scenarios as shown in Fig. 6 and the 3GPP members classify their measurements and simulations according to these sub-scenarios. Here we summarize the results of their measurements and simulations into Fig. 9 and Fig. 10.

Fig. 9 shows the range of parameters of the CI model for the InF scenario. In LOS cases, we can find that the path loss exponent varies from 1.8 to 2.4, and the shadow fading std varies from 1.9 to 5 dB. In NLOS cases, the exponent is in the range of 1.9 to 3.4, and the shadow fading std is in the range of 3.9 to 21 dB. Among the four sub-scenarios of NLOS, the link of the SH case shows the least blockage. Thus, its distance-dependent exponent is the smallest. While the DL case has the largest exponent with 3.4, which is due to the worst blockage situation. The DH case is the most complicated. Therefore, it shows the largest ranges for the shadow fading std and the distance-dependent exponent.

Because most of the measurements are only conducted at a particular frequency, we only summarize the parameters of the FI model here. The result is shown in Fig. 10. The marker size indicates the shadow fading std. There seems to be no visible trend considering the given parameter ranges. The intercept of LOS cases is from 30 to 71 dB, and the exponent is from 1.1 to 2.8. While the intercept of most NLOS cases is from 18 to 43 dB and the exponent is from 2.1 to 4.7. Among the four sub-scenarios, the DL case has the largest exponent. The intercepts of these four sub-scenarios are all below 55 dB.

After collecting the raw data of each sub-scenario [41], 3GPP TR 38.901 uses ABG model to specify the path loss models as the follows:

TABLE II
THE IMPACT OF CLUTTER DENSITY ON CI PATH LOSS MODEL [63]–[65].

	Frequency (GHz)	n[1]		σ (dB)[2]	
		sparse clutter	dense clutter	sparse clutter	dense clutter
LOS	1.3	1.79	1.79	4.55	4.42
	28	1.98	2.15	4.25	4.49
	60	2.05	1.91	4.53	3.99
	Average	1.94	1.95	4.44	4.3
NLOS	0.9	3.24	4.47	5.62	6.86
	1.3	2.38	2.81	4.67	8.09
	2.4	2.77	4.29	5.42	8.42
	5.2	2.18	3.7	4.93	5.15
	28	2.25	5.33	7.3	9.46
	60	2.35	5.67	6.29	10.07
	Average	2.53	4.38	5.71	8

[1] n is the distance-dependent path loss exponent in equation (3).
[2] σ is the shadow fading standard deviation.

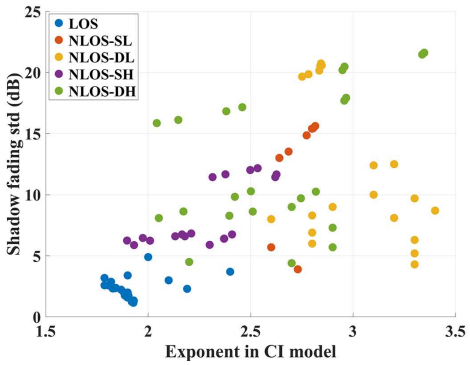

Fig. 9. The distribution of parameters in CI model [59], [66]–[69].

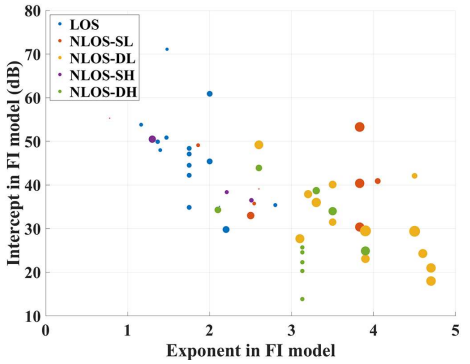

Fig. 10. The distribution of parameters in FI model [59], [61], [67]–[72]. The marker size represents the shadow fading std. The frequency of the model is from 1 to 100 GHz.

LOS case:

$$\begin{aligned}\mathrm{PL}_{\mathrm{LOS}}(f_c, d_{3\mathrm{D}}) &= 31.84 + 21.50\log_{10}(d_{3\mathrm{D}}) \\ &\quad +19.00\log_{10}(f_c), \sigma = 4.3\end{aligned} \tag{5}$$

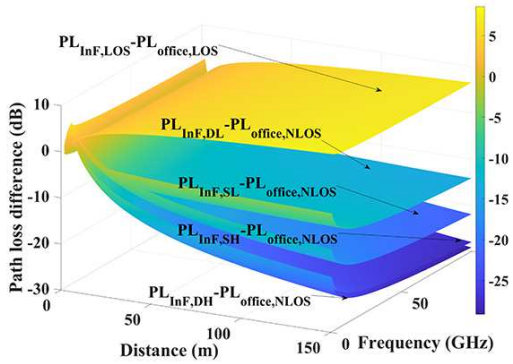

Fig. 11. Path loss difference between the InF and indoor office.

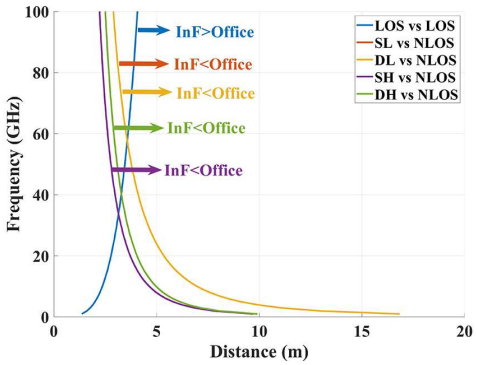

Fig. 12. Zero-boundary of path loss difference between the InF and indoor office.

NLOS-SL case:

$$\mathrm{PL}_{\mathrm{SL}}(f_c, d_{3\mathrm{D}}) = 33 + 25.5\log_{10}(d_{3\mathrm{D}}) + 20\log_{10}(f_c) \quad (6)$$

$$\mathrm{PL}_{\mathrm{NLOS}} = \max\left(\mathrm{PL}_{\mathrm{SL}}, \mathrm{PL}_{\mathrm{LOS}}\right), \ \sigma = 5.7 \quad (7)$$

NLOS-DL case:

$$\mathrm{PL}_{\mathrm{DL}}(f_c, d_{3\mathrm{D}}) = 18.6 + 35.7\log_{10}(d_{3\mathrm{D}}) + 20\log_{10}(f_c) \quad (8)$$

$$\mathrm{PL}_{\mathrm{NLOS}} = \max(\mathrm{PL}_{\mathrm{DL}}, \mathrm{PL}_{\mathrm{LOS}}, \mathrm{PL}_{\mathrm{SL}}), \ \sigma = 7.2 \quad (9)$$

NLOS-SH case:

$$\mathrm{PL}_{\mathrm{SH}}(f_c, d_{3\mathrm{D}}) = 32.4 + 23.0\log_{10}(d_{3\mathrm{D}}) + 20\log_{10}(f_c) \quad (10)$$

$$\mathrm{PL}_{\mathrm{NLOS}} = \max(\mathrm{PL}_{\mathrm{SH}}, \mathrm{PL}_{\mathrm{LOS}}), \ \sigma = 5.9 \quad (11)$$

NLOS-DH case:

$$\mathrm{PL}_{\mathrm{DH}}(f_c, d_{3\mathrm{D}}) = 33.63 + 21.9\log_{10}(d_{3\mathrm{D}}) + 20\log_{10}(f_c) \quad (12)$$

$$\mathrm{PL}_{\mathrm{NLOS}} = \max(\mathrm{PL}_{\mathrm{DH}}, \mathrm{PL}_{\mathrm{LOS}}), \ \sigma = 4.0 \quad (13)$$

We also compare the path loss models of the InF and indoor office. The difference of path loss in these two scenarios is driven by:

$$\mathrm{PL}_{\mathrm{diff}}(f_c, d_{3\mathrm{D}}) = \mathrm{PL}_{\mathrm{InF}} - \mathrm{PL}_{\mathrm{office}} \quad (14)$$

where $\mathrm{PL}_{\mathrm{InF}}$ and $\mathrm{PL}_{\mathrm{office}}$ represent the path loss models of InF and indoor office in LOS or NLOS cases. The result is shown in Fig. 11. We can find that $\mathrm{PL}_{\mathrm{diff}}(f_c, d_{3\mathrm{D}})$ increases with the frequency and distance in LOS case, but has the opposite tendency in NLOS cases. The zero-boundaries that divide the $\mathrm{PL}_{\mathrm{diff}}(f_c, d_{3\mathrm{D}})$ into the positive parts and negative parts are plotted in Fig. 12. All these zero-boundaries distribute below 20 m. If the maximum applicable distance is 150 m, then we can conclude that the InF has the larger LOS path loss and the smaller NLOS path loss within most application distances.

TABLE III
THE LOS PROBABILITY PARAMETERS [80].

Sub-scenarios	DH	MH[1]	SH	DL	ML[2]	SL
k_b	454	180	85	33	64	78
d_b	1	6.6	7	1	1	1
p_b	0.6	1	1	1	1	1

[1] medium density clutter, high BS (MH).
[2] medium density clutter, low BS (ML).

B. LOS probability

Setting the link condition is the second step in the channel coefficient generation procedure. The LOS probability model is used to determine whether the state of a channel is LOS or NLOS at a certain distance. In the traditional scenarios, such as UMi, UMa, Indoor office, and RMa, the LOS probability models are stochastic. Their forms are usually piecewise functions, whose first piece is a constant value (typical is 1) and the other parts consist of exponential functions [35].

Considering the NLOS case is always caused by blockage of machines in InF, some researchers suggest using the blockage model rather than a stochastic LOS probability model [73]. That means the LOS probability should be set to 100%. But more researchers suggest using a modified LOS probability model.

Because the clutter density and the antenna height also have a great impact on the LOS probability, the researchers introduce these two environment features when modelling the LOS probability [64], [74]–[79].

The [80] studies the impact of the BS antenna when modelling the LOS probability. It uses a two-piece model to describe LOS probability as:

$$\mathrm{Pr}_{\mathrm{LOS}}(d_{2\mathrm{D}}) = \begin{cases} p_b & d_{2\mathrm{D}} \le d_b, \\ \mathrm{e}^{\left(-\frac{d_{2\mathrm{D}} - d_b}{k_b}\right)} p_b & d_{2\mathrm{D}} > d_b. \end{cases} \quad (15)$$

Parameter $d_{2\mathrm{D}}$ is the 2-dimensional distance between the BS and UT. It can be found from Table III that k_b increases with the density of clutter when the BS antenna is higher than the clutter. When the BS antenna is lower than the average height of clutter, the relation between the clutter density and k_b becomes the opposite.

The effect of UT antenna height on LOS probability is studied in [69]. The distance between BS and UT is described by the 3-dimensional distance $d_{3\mathrm{D}}$. Fig. 13 is the simulation environment. The BS antenna height is 1.9 m, which is similar to the average height of clutter. The UT antenna height is set as 0.9 and 1.3 m respectively. The distribution of LOS

points is shown in Fig. 14. There are more LOS points in the black square area when the UT antenna height is 1.3 m. This is because the clutter is lower than the UT antenna in that area. The decreasing rate of LOS probability slows down accordingly. This phenomenon is also reflected in the model. When the UT antenna changes from clutter-embedded to clutter-elevated, the LOS probability model changes from a two-piece model (16) into a three-piece model (17), and the decreasing rate slows down in the third piece.

$$\mathrm{Pr}_{\mathrm{LOS}}(d_{\mathrm{3D}}) = \begin{cases} 1 & d_{\mathrm{3D}} \leq 4, \\ \mathrm{e}^{-\frac{d_{\mathrm{3D}}-4}{13.38}} & d_{\mathrm{3D}} > 4. \end{cases} \tag{16}$$

$$\mathrm{Pr}_{\mathrm{LOS}}(d_{\mathrm{3D}}) = \begin{cases} 1 & d_{\mathrm{3D}} \leq 4, \\ \mathrm{e}^{-\frac{d_{\mathrm{3D}}-4}{14.05}} & 4 < d_{\mathrm{3D}}, \\ \mathrm{e}^{-\frac{d_{\mathrm{3D}}-15}{28.23}} 0.457 & 15 < d_{\mathrm{3D}}. \end{cases} \tag{17}$$

When we want to model the LOS probability under different clutter densities, there are two alternatives. The first method is to dividing the environment into high and low density scenarios and fitting their LOS probability models as $\mathrm{Pr}_{\mathrm{LOS,high}}(d_{\mathrm{2D}})$ and $\mathrm{Pr}_{\mathrm{LOS,low}}(d_{\mathrm{2D}})$, respectively [64]. But this method is inconvenient when the environment clutter density is somewhere between the high and low density. To overcome this ambiguity in modelling, the second method introduces a weighting factor $W(r, d_{\mathrm{2D}})$ to assign the proportion of $\mathrm{Pr}_{\mathrm{LOS,high}}(d_{\mathrm{2D}})$ and $\mathrm{Pr}_{\mathrm{LOS,low}}(d_{\mathrm{2D}})$ in the model [78]. As shown in equation (18), the LOS probability $\mathrm{Pr}_{\mathrm{LOS}}(d_{\mathrm{2D}})$ can vary smoothly according to different cluster density r.

In the latest 3GPP 38.901 report, the LOS probability is defined as:

$$\mathrm{Pr}_{\mathrm{LOS,subsce}}(d_{\mathrm{2D}}) = \mathrm{e}^{-\frac{d_{\mathrm{2D}}}{k_{\mathrm{subsce}}}} \tag{19}$$

where

$$k_{\mathrm{subsce}} = \begin{cases} -\frac{d_{\mathrm{clutter}}}{\ln(1-r)} & \text{for subsce}\in \{\mathrm{SL}, \mathrm{DL}\}, \\ -\frac{d_{\mathrm{clutter}}}{\ln(1-r)} \frac{h_{\mathrm{BS}}-h_{\mathrm{UT}}}{h_c-h_{\mathrm{UT}}} & \text{for subsce}\in \{\mathrm{SH}, \mathrm{DH}\}. \end{cases} \tag{20}$$

This model is a one-piece model and it is derived for a canonical scenario as Fig. 15 [48], [81]. The value range of clutter density r is from 0 to 1. The parameters d_{clutter}, h_c, h_{UT}, h_{BS} are the clutter size, clutter height, antenna height of UT, and antenna height of BS. Comparing with the models in [69], [80], this model considers the clutter density and the antenna height at the same time. It is based on a deployment assumption rather than measurement data or ray-tracing simulation results. As a result, it may has some conflicts with the ray-tracing simulation results [82].

C. RMS delay spread

The time delay spread is important to any digital communication system. It can be easily obtained from any wide-band channel measurements.

The InF is an environment with abundant reflections. Many metallic machines with smooth surface diverse the propagation path of the signal. Correspondingly, the RMS delay spread in InF is larger than in the normal indoor office [83]–[88]. The RMS delay spread increases with increasing the proportion of MPCs in the environment [89], [90]. When the material of objects in the environment becomes electromagnetic absorbent, the RMS delay spread decreases from 664 ns to 10 ns in NLOS case [91].

To model the RMS delay spread in InF, 3GPP selected four candidate models: distance-dependent model, antenna-dependent model, frequency-dependent model, and volume-dependent model. The distance-dependent model is as shown in [15]:

$$\tau_{\mathrm{rms}} \propto d_{\mathrm{2D}}^{a} \tag{21}$$

where a is a constant and it can be deduced from the data fitting. But some researchers hold the opposite opinions [92]. The RMS delay spread also changes slightly with the height of the antenna [87], [93]. Its range is from 133.97 to 145.54 ns in LOS case and from 177.01 to 201.37 ns in NLOS case when the height of link changes from 0.9 to 2.5 m. But there is not enough research and data to support this antenna-dependent model, thus it is abandoned. The frequency-dependent model that is used in indoor office environments is a natural choice. But this is not suitable for InF anymore. The RMS delay spread seems not to change with the frequency in the simulation [88]. This leads to the absence of the frequency-dependent factor in the final model in 3GPP TR 38.901.

Some articles assume that the RMS delay spread is correlated with the factory volume V and the total surface area S. The total surface is the sum of the surface area of wall, ceiling, and floor. This modelling method is based on room electromagnetism (RE) that is borrowed from the field of room acoustics [94]. RE theory defines reverberation time as:

$$\tau_r = \frac{4V}{c\mu S} \tag{22}$$

where c is the speed of light in vacuum and μ is the median absorption coefficient. When the average power delay profile has an exponential decay, the τ_r equals the RMS delay spread [95]. Two assumptions needed to be satisfied when we use the RE model in InF scenario: the field's intensity does not depend on the direction (rich scattering environment) and its energy density is constant across the whole room (valid for rooms that are small enough). Inspired by the RE theory, [73] proposes a new model that establishes a relationship between the volume and the maximum observed RMS delay spread. Its improved edition is in [96], [97] and its final edition is as [98]:

$$\mathrm{Pr}_{\mathrm{LOS}}(r, d_{\mathrm{2D}}) = \begin{cases} p_b & d_{\mathrm{2D}} \leq d_b, \\ W(r, d_{\mathrm{2D}})\mathrm{Pr}_{\mathrm{LOS,low}}(d_{\mathrm{2D}}) + (1 - W(r, d_{\mathrm{2D}}))\mathrm{Pr}_{\mathrm{LOS,high}}(d_{\mathrm{2D}}) & d_{\mathrm{2D}} > d_b. \end{cases} \tag{18}$$

TABLE IV
FAST FADING PARAMETERS OF INDOOR AND INDOOR FACTORY [43].

Scenario		Indoor office		Indoor factory	
		LOS	NLOS	LOS	NLOS
Delay spread (DS)	μ_{lgDS}	$-0.01\log_{10}(1+f_c)-7.692$	$-0.28\log_{10}(1+f_c)-7.173$	$\log_{10}(26(\frac{V}{S})+14)-9.35$	$\log_{10}(30(\frac{V}{S})+32)-9.44$
$\text{lgDS}=\log_{10}(\text{DS}/1s)$	σ_{lgDS}	0.18	$0.1\log_{10}(1+f_c)+0.055$	0.15	0.19
AOD spread (ASD)	μ_{lgASD}	1.60	1.62	1.56	1.57
$\text{lgASD}=\log_{10}(\text{ASD}/1^\circ)$	σ_{lgASD}	0.18	0.25	0.25	0.2
AOA spread (ASA)	μ_{lgASA}	$-0.19\log_{10}(1+f_c)+1.781$	$-0.11\log_{10}(1+f_c)+1.863$	$-0.18\log_{10}(1+f_c)+1.78$	1.72
$\text{lgASA}=\log_{10}(\text{ASA}/1^\circ)$	σ_{lgASA}	$0.12\log_{10}(1+f_c)+0.119$	$0.12\log_{10}(1+f_c)+0.059$	$0.12\log_{10}(1+f_c)+0.2$	0.3
ZOA spread (ZSA)	μ_{lgZSA}	$-0.26\log_{10}(1+f_c)+1.44$	$-0.15\log_{10}(1+f_c)+1.387$	$-0.2\log_{10}(1+f_c)+1.5$	$-0.13\log_{10}(1+f_c)+1.45$
$\text{lgZSA}=\log_{10}(\text{ZSA}/1^\circ)$	σ_{lgZSA}	$-0.04\log_{10}(1+f_c)+0.264$	$-0.09\log_{10}(1+f_c)+0.746$	0.35	0.45
ZOD spread (ZSD)	μ_{lgZSD}	$-1.43\log_{10}(1+f_c)+2.228$	1.08	1.35	1.2
$\text{lgZSD}=\log_{10}(\text{ZSD}/1^\circ)$	σ_{lgZSA}	$0.13\log_{10}(1+f_c)+0.30$	0.36	0.35	0.55

[1] f_c is the center frequency in GHz.
[2] V is the volume in m^3, S is the total surface in m^2(walls+floor+ceiling).
[3] AOD: Azimuth angle Of Departure.
[4] AOA: Azimuth angle Of Arrival.
[5] ZOA: Zenith angle Of Arrival.
[6] ZOD: Zenith angle Of Departure.

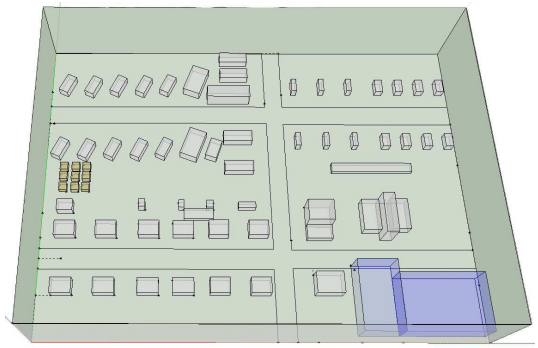

Fig. 13. The simulation environment in [69].

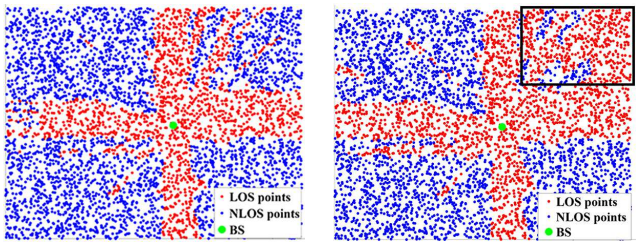

(a) UT antenna height is 0.9 m. (b) UT antenna height is 1.3 m.

Fig. 14. Distribution of LOS points in the environment of [69].

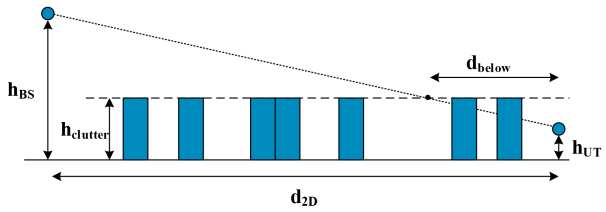

Fig. 15. The canonical geometry of one-piece model [48], [81].

LOS:

$$\mu_{\text{lgDS}}=\log_{10}(\frac{500}{6}\log_{10}(\max(V,1000))-200)-9.72 \quad (23)$$

NLOS:

$$\mu_{\text{lgDS}}=\log_{10}(\frac{500}{6}\log_{10}(\max(V,1000))-200)-9.42 \quad (24)$$

The std of both cases are 0.18.

From the results summarized by 3GPP, the RMS delay spread is supposed to be volume-dependent and it does not correlate with the frequency, distance, antenna height, and sub-scenario [99]. After summarizing a large number of references, [100] gives a more practical model which is based on the ratio of volume to the total surface, and it is adopted by 3GPP in Table IV.

D. Angular spread

The angular spread reflects the spatial characteristics of the wireless channel and it helps to design the MIMO system.

According to the current studies, the volume of the factory hall mainly affects the angular spread [100], [101]. This phenomenon is more obvious for Azimuth angle Spread of Arrival (ASA) in LOS case, because the ASA increases with the distance [102].

The angular spread also increases with the number of MPCs and the density of the clutter [64], [84]. As the clutter density changes from low to high, the ASA increases by about 10° to 37°, and the Azimuth angle Spread of Departure (ASD) increases by about 30°. Besides, the angular spread shows the frequency-dependent behavior [86], [100], which leads to the frequency-dependent model in 3GPP TR 38.901. Unfortunately, there are few papers about the angular spread in InF scenarios and most of them are about the ASA. Hence, the angular characteristics modelling in InF scenarios need further study. In Fig. 16, we plot some measured ASA of the reference papers. Considering that some referenced paper do not provide the mean value of the ASA but only the value range, we use dotted lines to represent the value ranges in the figure. From Table IV, Fig. 16 and Fig. 17 we can find the ASA, Zenith angle Spread of Arrival (ZSA) and Zenith angle Spread of Departure (ZSD) are larger in InF for most frequency bands. But the ASD is larger in the indoor office scenario.

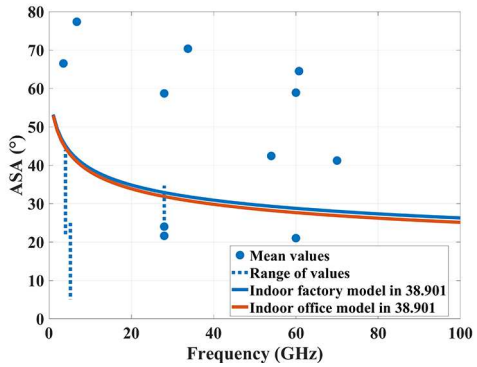

(a) ASA in LOS case.

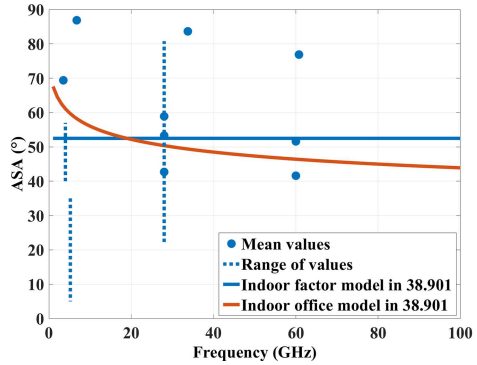

(b) ASA in NLOS case.

Fig. 16. Distribution of ASA values in references [64], [70], [84], [86], [102]–[104].

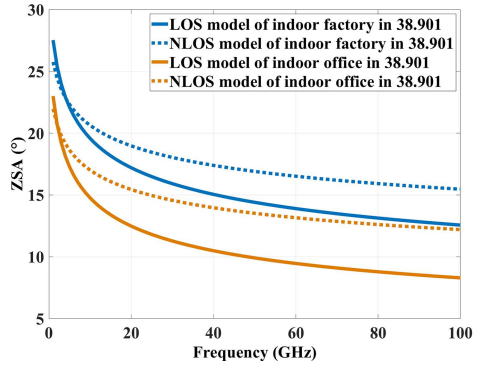

Fig. 17. ZSA model in 3GPP TR 38.901.

E. Dual mobility

In industrial facilities, there may exist random/periodic movements of workers, robots, trucks, overhead cranes, suspended equipment, or other objects, which could cause time-varying channel conditions. To model these conditions, 3GPP TR 38.901 adds the dual mobility model in the InF scenarios [105].

The dual mobility is not a new concept in the channel model. It has been modelled in 3GPP TR 37.885 [106] which is for the Vehicle-to-everything (V2X) scenarios. As suggested in the proposal [107], [108], 3GPP TR 38.901 model directly borrows the dual mobility model from 3GPP TR 37.885 standard model as a new part. In the dual mobility model, the Doppler for the mth LOS path in the lth cluster is shown as equation (25):

$$\nu_{l,m} = \frac{\hat{r}^T_{\mathrm{rx},l,m}\bar{\nu}_{\mathrm{rx}} + \hat{r}^T_{\mathrm{tx},l,m}\bar{\nu}_{\mathrm{tx}}}{\lambda_0} \tag{25}$$

The parameter λ_0 is the wavelength of carrier frequency. $\hat{r}^T_{\mathrm{rx},l,m}$ and $\hat{r}^T_{\mathrm{tx},l,m}$ are direction vectors of arrival and departure paths. $\bar{\nu}_{\mathrm{rx}}$ and $\bar{\nu}_{\mathrm{tx}}$ are the movement direction vectors of receiver and transmitter respectively. They are written as:

$$\bar{\nu}_{\mathrm{rx}} = \nu_{\mathrm{rx}} \begin{bmatrix} \sin\theta_{\nu,\mathrm{rx}}\cos\phi_{\nu,\mathrm{rx}} \\ \sin\theta_{\nu,\mathrm{rx}}\sin\phi_{\nu,\mathrm{rx}} \\ \cos\theta_{\nu,\mathrm{rx}} \end{bmatrix} \tag{26}$$

$$\bar{\nu}_{\mathrm{tx}} = \nu_{\mathrm{tx}} \begin{bmatrix} \sin\theta_{\nu,\mathrm{tx}}\cos\phi_{\nu,\mathrm{tx}} \\ \sin\theta_{\nu,\mathrm{tx}}\sin\phi_{\nu,\mathrm{tx}} \\ \cos\theta_{\nu,\mathrm{tx}} \end{bmatrix} \tag{27}$$

For all other paths, the Doppler frequency component is given by equation (28):

$$\nu_{l,m} = \frac{\hat{r}^T_{\mathrm{rx},l,m}\bar{\nu}_{\mathrm{rx}} + \hat{r}^T_{\mathrm{tx},l,m}\bar{\nu}_{\mathrm{tx}} + 2\alpha_{l,m}D_{l,m}}{\lambda_0} \tag{28}$$

where $D_{l,m}$ is a random variable from $-\nu_{\mathrm{scatt}}$ to ν_{scatt}, and ν_{scatt} is the maximum speed of the clutter in the environment. But note here that $D_{l,m}$ is not uniformly distributed as described in 3GPP TR 37.885 standard model. Since there are not many related studies in InF, the distribution of $D_{l,m}$ still needs to be studied in the future. The parameter $\alpha_{l,m}$ is a Bernoulli distributed random variable with the mean value of 0.2, which is different from obeying uniform distribution in 3GPP TR 37.885 standard model. This is because the majority of the scattering objects, such as walls, floors, ceiling, shelves, equipment, etc., are stationary in InF. The two-state Bernoulli distribution is enough to describe the movement of the objects, and the distribution of these Doppler shifts can be very different from a V2X scenario [108].

F. Absolute time of arrival

One of the key requirements in many industrial use-cases is precise positioning, e.g., in motion planning of robotic arms/AGVs, locating assets in warehouses, etc [76]. While in the previous channel model, the delay of the first arriving path was defined as zero. This is not enough to determine the exact position. The new model needs to add the absolute time of arrival to evaluate the position of moving BS/UT [77].

The discussions about absolute time of arrival are divided into the LOS case and the NLOS case. In the LOS case, the absolute time of arrival is calculated from the propagation distance of the direct path as:

$$\tau_{\mathrm{abs,LOS}} = \frac{d_{\mathrm{3D}}}{c} \tag{29}$$

where d_{3D} is the 3-dimension distance between BS and UT. In the NLOS case, the absolute time is defined as the sum of $\tau_{\mathrm{abs,LOS}}$ and $\Delta\tau$:

$$\tau_{\mathrm{abs,NLOS}} = \frac{d_{\mathrm{3D}}}{c} + \Delta\tau, \Delta\tau > 0 \tag{30}$$

TABLE V
PARAMETER FOR THE ABSOLUTE TIME OF ARRIVAL MODEL IN INDOOR FACTORY [43].

Sub-scenario		SL, DL	SH, DH
$\lg\Delta\tau = \log_{10}(\Delta\tau/1s)$	$\mu_{\lg\Delta\tau}$	-7.5	-7.5
	$\sigma_{\lg\Delta\tau}$	0.4	0.4
Correlation distance in the horizontal plane [m]		6	11

During the discussion at 3GPP conferences, most 3GPP members agree on the equation (29) but propose different modelling methods for $\Delta\tau$ in NLOS case. In [109], the $\Delta\tau$ is defined as:

$$\Delta\tau = \min(10^{\tau_{\mathrm{dif}}}, \tau^{\mathrm{lim}}) \tag{31}$$

where τ^{lim} is related to the maximum measurable propagation distance but it was deleted in [110]. The new edition of $\Delta\tau$ is written as:

$$\Delta\tau = 10^{\tau_{\mathrm{dif}}} \tag{32}$$

The parameter τ_{dif} is normally distributed and it is defined as:

$$\tau_{\mathrm{dif}} = \lg(\tau^{\mathrm{st}}_{\mathrm{NLOS}} - \tau_{\mathrm{abs,LOS}}) \tag{33}$$

The $\tau^{\mathrm{st}}_{\mathrm{NLOS}}$ is the absolute time of first arrival NLOS path. The mean values of τ_{dif} are -7.47 (33.9 ns) and -8.43 (3.7 ns) respectively in the low and high BS sub-scenarios.

In [111] $\Delta\tau$ is assumed to follow Gaussian distribution with truncation so that $\Delta\tau > 0$. Its mean value is 55 ns and the standard deviation is 28 ns in low BS sub-scenario. But this assumption was adjusted to a log-normal distribution in [112]. In [113], [114] $\Delta\tau$ is defined as:

$$\Delta\tau = Y \cdot \tau_{\mathrm{abs,LOS}} \tag{34}$$

where Y is a random variable with an exponential distribution function of:

$$p_Y(y) = xe^{-xy} \tag{35}$$

The x is a scenario-dependent scaling parameter, and it is assumed to be 5 and 2 in SL and DL sub-scenarios, respectively [115].

To evaluate the accuracy of the three distributions (log-normal, Gaussian, exponential) of $\Delta\tau$, [116] tested the minimum fitting error of them. The results suggested using the log-normal distribution in low BS sub-scenarios and exponential distribution in high BS sub-scenarios is a better choice.

Another method to model the absolute time of arrival is proposed in [105]. It assumes the paths are the single-bounce propagation and calculate the absolute delay by the angular distributions. But in the present channel model standards, the single-bounce propagation path is not the precondition of the fitting distributions of AoDs and AoAs; thus, it may have conflicts with the real environment.

At last, the equations (29) and (30) are decided as the absolute time of arrival in the latest 3GPP TR 38.901. $\Delta\tau$ is generated from a log-normal distribution with parameters according to Table V and its maximum value is $2L/c$, where L is the largest dimension of the factory hall, i.e. $L = \max(\mathrm{length}, \mathrm{width}, \mathrm{height})$ [117].

VI. OTHER CHANGES IN THE IIOT MODEL

In addition to the path loss, LOS probability, delay spread, angular spread, dual mobility, and absolute time of arrival, the new 3GPP TR 38.901 standard channel model has some other changes.

In the out-to-indoor (O2I) part, the InF scenario is suggested using the high penetration loss model. Besides, considering that the cluster number increases to 25 in the InF scenario, the angular generation scaling factors also change accordingly. The AoA and AoD generation scaling factor for 25 clusters is defined as 1.358. The ZoA and ZoD generation scaling factor for 25 clusters is defined as 1.282.

In the spatial consistency part, the correlation distance for the cluster and ray specific random variables is defined as 10 m in the InF scenario. The correlation distance for LOS and NLOS state is defined to $d_{\mathrm{clutter}}/2$. d_{clutter} is the clutter size. The BS mobility is also considered in the spatial consistent mobility modelling.

As for the blockage model, the AGV and robot are identified as the typical blockers in InF. Their blockage model is type B. The size of AGV is 3 m$\times$1.5 m (width$\times$height) and the size of robot is 2 m$\times$0.2 m. The moving speed of AGV is up to 30 km/h, and the moving speed of the robot is up to 3 m/s.

VII. CONCLUSION AND FUTURE WORK

This article introduces the first standardized 5G IIoT channel model released by 3GPP. Because the IIoT scenarios have amount of metal machines, their huge bodies and the smooth metal surfaces complicate the radio signal propagation. To describe the wireless environment in a more precise way, this new IIoT model considers environment features, such as the clutter density, antenna height, factory volume and the total surface when modelling the large-scale and small-scale parameters. Moreover, to meet the requirement for the movement and the positioning in IIoT scenarios, the dual mobility and the absolute time of arrival are added in this model. Although researchers have done a lot of work on this aspect, there are still some problems to be solved. Due to lack of the measurement data, most fast fading parameters in the model are just initial values. The Omitting of Dense Multipath Components (DMCs) from model could result into an underestimation of the received power and the richness of multipath. Establishing the standardized IIoT channel model is just a beginning. More and more research focused in this scenario will perfect this IIoT channel model. We hope this paper can provide some new thoughts for future works.

APPENDIX A

The important abbreviations in this paper are listed in Table VI.

ACKNOWLEDGMENT

The 3GPP work is a collaborative effort of persons from many different affiliations. The authors are grateful to acknowledge Prasanth Karunakaran [Fraunhofer IIS], Bolun Guo [Huawei], Frank Hsieh [Nokia], Ignacio Rodriguez Larrad

TABLE VI
ABBREVIATIONS IN THIS PAPER.

Abbreviations	Full forms
3GPP	3rd Generation Partnership Project
5G	Fifth-Generation
5G-ACIA	5G Alliance for Connected Industries and Automation
ABG model	Alpha-beta-gamma path loss model
AGVs	Automatic Guided Vehicles
AOA	Azimuth angle Of Arrival
AOD	Azimuth angle Of Departure
ASA	Azimuth angle Spread of Arrival
ASD	Azimuth angle Spread of Departure
BS	Base Station
CI model	Close-in free space model
D2D	Device-to-device
DH	Dense clutter, High BS
DL	Dense clutter, Low BS
DS	Delay Spread
eMBB	Enhanced Mobile Broadband
FI model	Floating-intercept model
GSCM	Geometry-based Stochastic Channel Model
gNB	gNodeB
IF	Indoor Factory
IIoT	Industrial Internet of Things
InH	Indoor Hotspot
ISM	Industrial, Scientific, Medical
ITU	International Telecommunication Union
LOS	Line-of-sight
MEC	Mobile/Multi-access Edge Computing
MH	Medium density clutter, High BS
MIMO	Multiple-Input Multiple-Output
ML	Medium density clutter, Low BS
MMSE	Minimum Mean Square Error
mMTC	Massive Machine Type Communication
NLOS	Nonline-of-sight
RAN	Radio Access Network
RAN1	Radio Access Network Working Group 1
RE	room electromagnetism
RMa	Rural Macro
RMS	Root Mean Square
SH	Sparse clutter, High BS
SL	Sparse clutter, Low BS
TSG	Technical Specification Group
UMa	Urban Macro
UMi	Urban Micro
URLLC	Ultra-reliable and Low Latency Communication
UT	User Terminal
UWB	Ultra-wideband
V2X	Vehicle-to-everything
ZOA	Zenith angle Of Arrival
ZOD	Zenith angle Of Departure
ZSA	Zenith angle Spread of Arrival
ZSD	Zenith angle Spread of Departure

[Aalborg University], Koshiro Kitao [NTT DOCOMO], Piyush Gupta [Qualcomm] for their strong support to the channel modelling work.

The work of the BUPT authors is supported by the Project from Outstanding Youth Fund of National Natural Science Foundation of China (Grant No.61925102), National Key R&D Program of China (Grant No.2018YFE020550), the Key Program of Beijing Municipal Natural Science Foundation (Grant No.L172030), and ZTE corporation.

REFERENCES

[1] J. Karlsson, "5G for Business: A 2030 Market Compass," Ericsson, Business Potential Report, Oct. 2019. [Online]. Available: https://www.ericsson.com/en/5g/5g-for-business/5g-for-business-a-2030-market-compass

[2] K. Cambell, J. Diffiey, B. Flanagan, B. Morelli, B. O'Neil, and F. Sideco, "The 5G Economy: How 5G Technology Will Contribute to the Globe Economy," IHS Economics/IHS Technology, Business Potential Report, Jan. 2017.

[3] W. Li, X. Hu, and T. Jiang, "Path Loss Models for IEEE 802.15.4 Vehicle-to-Infrastructure Communications in Rural Areas," *IEEE Internet of Things Journal*, vol. 5, no. 5, pp. 3865–3875, Jun. 2018.

[4] W. Xu, J. Y. Kim, W. Huang, S. S. Kanhere, S. K. Jha, and W. Hu, "Measurement, Characterization, and Modeling of LoRa Technology in Multifloor Buildings," *IEEE Internet of Things Journal*, vol. 7, no. 1, pp. 298–310, Oct. 2020.

[5] S. Fu and H. Z. J.Chen, "Time Sensitive Networking Technology Overview and Performance Analysis," *ZTE Communications*, vol. 16, no. 4, pp. 57–64, Oct. 2018.

[6] W. Li, J. Zhang, X. Ma, Y. Zhang, H. Huang, and Y. Cheng, "The Way to Apply Machine Learning to IoT Driven Wireless Network from Channel Perspective," *China Communications*, vol. 16, no. 1, pp. 148–164, Jan. 2019.

[7] J. Zhang, P. Tang, L. Yu, T. Jiang, and L. Tian, "Channel Measurements and Models for 6G: Current Status and Future Outlook," *Frontiers of Information Technology and Electronic Engineering*, vol. 21, no. 1, pp. 39–61, year=2020, month=Mar., publisher=Zhejiang University Press and Springer, doi=10.1631/FITEE.1 900 450.

[8] H. Lu, X. Li, R. Xie, and W. Feng, "Integrated Architecture for Networking and Industrial Internet Identity," *ZTE Communications*, vol. 18, no. 1, pp. 24–35, Mar. 2020.

[9] T. S. Rappaport, S. Y. Seidel, and K. Takamizawa, "Statistical Channel Impulse Response Models for Factory and Open Plan Building Radio Communicate System Design," *IEEE Transactions on Communications*, vol. 39, no. 5, pp. 794–807, May 1991.

[10] T. S. Rappaport and C. D. McGillem, "Characterising the UHF Factory Radio Channel," *Electronics Letters*, vol. 23, no. 19, pp. 1015–1017, Sep. 1987.

[11] T. S. Rappaport and C. D. McGillem, "UHF Fading in Factories," *IEEE Journal on Selected Areas in Communications*, vol. 7, no. 1, pp. 40–48, Jan. 1989.

[12] T. S. Rappaport, "Characterization of UHF Multipath Radio Channels in Factory Buildings," *IEEE Transactions on Antennas and Propagation*, vol. 37, no. 8, pp. 1058–1069, Aug. 1989.

[13] A. F. Molisch, K. Balakrishnan, D. Cassioli, C. Chong, S. Emami, A. Fort, J. Karedal, J. Kunisch, H. Schantz, U. Schuster, and K. Siwiak, "IEEE 802.15.4a Channel Model - Final Report," vol. 15, Jan. 2004.

[14] A. F. Molisch, D. Cassioli, C. Chong, S. Emami, A. Fort, B. Kannan, J. Karedal, J. Kunisch, H. G. Schantz, K. Siwiak, and M. Z. Win, "A Comprehensive Standardized Model for Ultrawideband Propagation Channels," *IEEE Transactions on Antennas and Propagation*, vol. 54, no. 11, pp. 3151–3166, Nov. 2006.

[15] J. Karedal, S. Wyne, P. Almers, F. Tufvesson, and A. F. Molisch, "A Measurement-Based Statistical Model for Industrial Ultra-Wideband Channels," *IEEE Transactions on Wireless Communications*, vol. 6, no. 8, pp. 3028–3037, Aug. 2007.

[16] E. I. Adegoke, R. M. Edwards, W. G. Whittow, and A. Bindel, "Characterizing the Indoor Industrial Channel at 3.5 GHz for 5G," in *2019 Wireless Days (WD)*, Apr. 2019, pp. 1–4.

[17] Y. Ai, M. Cheffena, and Q. Li, "Radio Frequency Measurements and Capacity Analysis for Industrial Indoor Environments," in *2015 9th European Conference on Antennas and Propagation (EuCAP)*, Apr. 2015, pp. 1–5.

[18] Y. Ai, M. Cheffena, and Q. Li, "Power Delay Profile Analysis and Modeling of Industrial Indoor Channels," in *2015 9th European Conference on Antennas and Propagation (EuCAP)*, Apr. 2015, pp. 1–5.

[19] M. A. Matin, K. A. Yasmeen, M. A. Mohd Ali, A. K. M. Wahiduzzaman, and A. Imtiaz, "Statistical Model for UWB Channel in an Industrial Environment," in *2008 International Conference on Microwave and Millimeter Wave Technology*, vol. 2, Apr. 2008, pp. 1015–1017.

[20] A. Traßl, T. Hößler, L. Scheuvens, N. Franchi, and G. P. Fettweis, "Deriving an Empirical Channel Model for Wireless Industrial Indoor Communications," in *2019 IEEE 30th Annual International Symposium on Personal, Indoor and Mobile Radio Communications (PIMRC)*, Sep. 2019, pp. 1–7.

[21] K. Zhang, L. Liu, C. Tao, Z. Yuan, and J. Zhang, "Channel Measurement and Characterization for Industrial Internet of Things," in *2019 IEEE Wireless Communications and Networking Conference (WCNC)*, Apr. 2019, pp. 1–5.

[22] S. Jaeckel, N. Turay, L. Raschkowski, L. Thiele, R. Vuohtoniemi, M. Sonkki, V. Hovinen, F. Burkhardt, P. Karunakaran, and T. Heyn, "Industrial Indoor Measurements from 2-6 GHz for the 3GPP-NR and QuaDRiGa Channel Model," in *2019 IEEE 90th Vehicular Technology Conference (VTC2019-Fall)*, Sep. 2019, pp. 1–7.

[23] L. Liu, K. Zhang, C. Tao, K. Zhang, Z. Yuan, and J. Zhang, "Channel Measurements and Characterizations for Automobile Factory Environments," in *2018 20th International Conference on Advanced Communication Technology (ICACT)*, Feb. 2018, pp. 234–238.

[24] J. Yang, B. Ai, I. You, M. Imran, L. Wang, K. Guan, D. He, Z. Zhong, and W. Keusgen, "Ultra-Reliable Communications for Industrial Internet of Things: Design Considerations and Channel Modeling," *IEEE Network*, vol. 33, no. 4, pp. 104–111, Jul. 2019.

[25] ITU-R, "Guidelines for Evaluation of Radio Interface Technologies for IMT-2020," International Telecommunication Union, Technical Report M.2412-0, Oct. 2017. [Online]. Available: https://www.itu.int/pub/R-REP-M.2412-2017

[26] 3GPP, "Study on Channel Model for Frequencies from 0.5 to 100 GHz," 3rd Generation Partnership Project, Technical Report TR 38.901 V15.0.0, Jun. 2018. [Online]. Available: https://portal.3gpp.org/desktopmodules/Specifications/SpecificationDetails.aspx?specificationId=3173

[27] L. Liu, C. Oestges, J. Poutanen, K. Haneda, P. Vainikainen, F. Quitin, F. Tufvesson, and P. D. Doncker, "The COST 2100 MIMO Channel Model," *IEEE Wireless Communications*, vol. 19, no. 6, pp. 92–99, Dec. 2012.

[28] L. Raschkowski, P. Kyösti, K. Kusume, T. Jämsä, V. Nurmela, A. Karttunen, A. Roivainen, T. Imai, J. Järveläinen, J. Medbo, J. Vihriälä, J. Meinilä, K. Haneda, V. Hovinen, J. Ylitalo, N. Omaki, A. Hekkala, R. Weiler, and M. Peter, "METIS Channel Models," METIS, Technical Report ICT-317669-METIS/D1.4, Jul. 2015, third Edition.

[29] M. Peter, K. Haneda, S. L. H. Nguyen, A. Karttunen, J. Järveläinen, A. Bamba, R. D'Errico, J. Medbo, F. Undi, S. Jaeckel, N. Iqbal, J. Luo, M. Rybakowski, C. Diakhate, J. Conrat, A. Naehring, S. Wu, A. Goulianos, and E. Mellios, "Measurement Results and Final mmMAGIC Channel Models," mmMAGIC, Technical Report H2020-ICT-671650-mmMAGIC/D2.2, May 2017, second Edition.

[30] S. Sun, G. R. MacCartney, and T. S. Rappaport, "A Novel Millimeter-wave Channel Simulator and Applications for 5G Wireless Communications," in *2017 IEEE International Conference on Communications (ICC)*, Jul. 2017, pp. 1–7.

[31] S. Jaeckel, L. Raschkowski, K. Börner, L. Thiele, F. Burkhardt, and E. Eberlein, "Quasi Deterministic Radio Channel Generator User Manual and Documentation," Fraunhofer Heinrich Hertz Institute, Technical Report v2.2.0, Jun. 2019.

[32] J. Zhang, C. Pan, F. Pei, G. Liu, and X. Cheng, "Three-Dimensional Fading Channel Models: A Survey of Elevation Angle Research," *IEEE Communications Magazine*, vol. 52, no. 6, pp. 218–226, Jun. 2014.

[33] J. Zhang, Y. Zhang, Y. Yu, R. Xu, Q. Zheng, and P. Zhang, "3-D MIMO: How Much Does It Meet Our Expectations Observed From Channel Measurements?" *IEEE Journal on Selected Areas in Communications*, vol. 35, no. 8, pp. 1887–1903, Jun. 2017.

[34] L. Tian, J. Zhang, H. Tan, P. Tang, and G. Liu, "Propagation Characteristics of Elevation Angles and Three Dimensional Fading Channel Model with Angle Offset," *China Communications*, vol. 16, no. 9, pp. 62–78, Sep. 2019.

[35] 3GPP, "Study on Channel Model for Frequencies from 0.5 to 100 GHz," 3rd Generation Partnership Project, Technical Report TR 38.901 V16.0.0, Oct. 2019. [Online]. Available: https://portal.3gpp.org/desktopmodules/Specifications/SpecificationDetails.aspx?specificationId=3173

[36] M. Mahbub, "Comparative Link-level Analysis and Performance Estimation of Channel Models for IIoT (Industrial-IoT) Wireless Communications," *Internet of Things*, vol. 12, p. 100315, Dec. 2020.

[37] M. Cheffena, "Propagation Channel Characteristics of Industrial Wireless Sensor Networks [Wireless Corner]," *IEEE Antennas and Propagation Magazine*, vol. 58, no. 1, pp. 66–73, Mar. 2016.

[38] W. Wang, S. L. Capitaneanu, D. Marinca, and E. Lohan, "Comparative Analysis of Channel Models for Industrial IoT Wireless Communication," *IEEE Access*, vol. 7, pp. 91 627–91 640, Jul. 2019.

[39] Ericsson, "New SI Proposal: Study on Channel Modeling for Indoor Industrial Scenarios," 3rd Generation Partnership Project, Proposal RP-182138, Sep. 2018. [Online]. Available: https://www.3gpp.org/DynaReport/TDocExMtg--RP-81--18666.htm

[40] Ericsson, "List of Agreements," 3rd Generation Partnership Project, Proposal R1-1909333, Aug. 2019. [Online]. Available: https://www.3gpp.org/ftp/tsg_ran/WG1_RL1/TSGR1_98/Docs/

[41] Ericsson, Fraunhofer HHI, and Fraunhofer IIS, "List of Measurements," 3rd Generation Partnership Project, Proposal R1-1909706, Aug. 2019. [Online]. Available: https://www.3gpp.org/ftp/tsg_ran/WG1_RL1/TSGR1_98/Docs/

[42] Ericsson, NTT DOCOMO, Nokia, CEA-LETI, Fraunhofer HHI, and Fraunhofer IIS, "Addition of Indoor Industrial Channel Model," 3rd Generation Partnership Project, Proposal R1-1909807, Aug. 2019. [Online]. Available: https://www.3gpp.org/ftp/tsg_ran/WG1_RL1/TSGR1_98/Docs/

[43] 3GPP, "Study on Channel Model for Frequencies from 0.5 to 100 GHz," 3rd Generation Partnership Project, Technical Report TR 38.901 V16.1.0, Dec. 2019. [Online]. Available: https://portal.3gpp.org/desktopmodules/Specifications/SpecificationDetails.aspx?specificationId=3173

[44] Huawei and HiSilicon, "CR to TR 38.901 for Remaining Open Issues in IIoT Channel Modelling," 3rd Generation Partnership Project, Proposal R1-1911670, Oct. 2019. [Online]. Available: https://portal.3gpp.org/desktopmodules/Specifications/SpecificationDetails.aspx?specificationId=3173

[45] B. Hanssens, S. R. Kshetri, E. Tanghe, D. Plets, J. Hoebeke, A. Karaağaç, J. Haxhibeqiri, D. P. Gaillot, M. Liénard, C. Oestges, L. Martens, and W. Joseph, "Measurement-Based Analysis of Dense Multipath Components in a Large Industrial Warehouse," in *12th European Conference on Antennas and Propagation (EuCAP 2018)*, Apr. 2018, pp. 1–5.

[46] T. Jiang, L. Tian, J. Zhang, Y. Zheng, Q. Wang, and J. Dou, "The Impact of Antenna Height on the Channel Model in Indoor Industrial Scenario," in *2020 IEEE/CIC International Conference on Communications in China (ICCC Workshops)*, Aug. 2020, pp. 1–6.

[47] Huawei and HiSilicon, "Sub-scenario Specific Path Loss Models for IIoT," 3rd Generation Partnership Project, Proposal R1-1908072, Aug. 2019. [Online]. Available: https://www.3gpp.org/ftp/tsg_ran/WG1_RL1/TSGR1_98/Docs/

[48] Ericsson, "Summary of Email Discussion on Indoor Industrial Channel Model and Calibration," 3rd Generation Partnership Project, Proposal R1-1907968, Aug. 2019. [Online]. Available: https://www.3gpp.org/ftp/tsg_ran/WG1_RL1/TSGR1_98/Docs/

[49] 5G-ACIA, "LS on Channel Model for Indoor Industrial Scenarios," 3rd Generation Partnership Project, Proposal RP-181521, Sep. 2018. [Online]. Available: https://www.3gpp.org/DynaReport/TDocExMtg--RP-81--18666.htm

[50] ITU, "Radio Regulations," Articles ITU R RR (2016), 2016. [Online]. Available: https://www.itu.int/pub/R-REG-RR-2016

[51] N. A. A. Syed and P. J. Green, "Wideband Communication Channel Sounding for Wireless Industrial Internet-of-Things Applications," in *2019 IEEE VTS Asia Pacific Wireless Communications Symposium (APWCS)*, Aug. 2019, pp. 1–5.

[52] S. Savazzi, V. Rampa, and U. Spagnolini, "Wireless Cloud Networks for the Factory of Things: Connectivity Modeling and Layout Design," *IEEE Internet of Things Journal*, vol. 1, no. 2, pp. 180–195, Jun. 2014.

[53] Ericsson, "Email Discussion on Frequency Bands of Interest," 3rd Generation Partnership Project, Proposal R1-1903123, Feb. 2019. [Online]. Available: https://www.3gpp.org/ftp/tsg_ran/WG1_RL1/TSGR1_96/Docs/

[54] Ericsson, "Views on Scenario Description, Frequency Bands of Interest, and Existing Literature on Channel Measurements for the Indoor Industrial Scenario," 3rd Generation Partnership Project, Proposal R1-1813129, Nov. 2018. [Online]. Available: https://www.3gpp.org/ftp/tsg_ran/WG1_RL1/TSGR1_95/Docs/

[55] Huawei and HiSilicon, "Survey of Frequency Band of Interest for Industrial IoT," 3rd Generation Partnership Project, Proposal R1-1813671, Nov. 2018. [Online]. Available: https://www.3gpp.org/ftp/tsg_ran/WG1_RL1/TSGR1_95/Docs/

[56] F. Huang, L. Tian, Y. Zheng, and J. Zhang, "Propagation Characteristics of Indoor Radio Channel from 3.5 GHz to 28 GHz," in *2016 IEEE 84th Vehicular Technology Conference (VTC-Fall)*, Sep. 2016, pp. 1–5.

[57] S. Sun, T. A. Thomas, T. S. Rappaport, H. Nguyen, I. Z. Kovacs, and I. Rodriguez, "Path Loss, Shadow Fading, and Line-of-Sight Probability Models for 5G Urban Macro-Cellular Scenarios," in *2015 IEEE Globecom Workshops (GC Wkshps)*, Dec. 2015, pp. 1–7.

[58] T. S. Rappaport, G. R. MacCartney, M. K. Samimi, and S. Sun, "Wideband Millimeter-Wave Propagation Measurements and Channel Models for Future Wireless Communication System Design," *IEEE Transactions on Communications*, vol. 63, no. 9, pp. 3029–3056, May 2015.

[59] Nokia and Nokia Shanghai Bell, "Path Loss Data Analysis and Model Proposal for the Different Indoor Industrial Sub-scenarios," 3rd Generation Partnership Project, Proposal R1-1909002, Aug. 2019. [Online]. Available: https://www.3gpp.org/ftp/tsg_ran/WG1_RL1/TSGR1_98/Docs/

[60] ZTE and Sanechips, "LOS Probability Model in IIoT Scenario," 3rd Generation Partnership Project, Proposal R1-1908313, Aug. 2019. [Online]. Available: https://www.3gpp.org/ftp/tsg_ran/WG1_RL1/TSGR1_98/Docs/

[61] CMCC and BUPT, "New Measurements and Modelling on Pathloss in IIoT Scenarios," 3rd Generation Partnership Project, Proposal R1-1904742, Apr. 2018. [Online]. Available: https://www.3gpp.org/ftp/tsg_ran/WG1_RL1/TSGR1_96b/Docs/

[62] Nokia and Nokia Shanghai Bell, "Scenarios, Frequencies and New Field Measurement Results from Two Operational Factory Halls at 3.5 GHz for Various Antenna Configurations," 3rd Generation Partnership Project, Proposal R1-1813177, Nov. 2018. [Online]. Available: https://www.3gpp.org/ftp/tsg_ran/WG1_RL1/TSGR1_95/Docs/

[63] T. S. Rappaport, "Indoor Radio Communications for Factories of the Future," *IEEE Communications Magazine*, vol. 27, no. 5, pp. 15–24, May 1989.

[64] D. Solomitckii, A. Orsino, S. Andreev, Y. Koucheryavy, and M. Valkama, "Characterization of mmWave Channel Properties at 28 and 60 GHz in Factory Automation Deployments," in *2018 IEEE Wireless Communications and Networking Conference (WCNC)*, Apr. 2018, pp. 1–6.

[65] E. Tanghe, W. Joseph, L. Verloock, L. Martens, H. Capoen, K. V. Herwegen, and W. Vantomme, "The Industrial Indoor Channel: Large-scale and Temporal Fading at 900, 2400, and 5200 MHz," *IEEE Transactions on Wireless Communications*, vol. 7, no. 7, pp. 2740–2751, Jul. 2008.

[66] Huawei and HiSilicon, "Preliminary Channel Measurement on Large-Scale Propagation Loss for Indoor Factory Environment," 3rd Generation Partnership Project, Proposal R1-1906620, May 2019. [Online]. Available: https://www.3gpp.org/ftp/tsg_ran/WG1_RL1/TSGR1_97/Docs/

[67] Nokia and Nokia Shanghai Bell, "Extended Path Loss Parametrization Analysis from Measurements in Two Operational Factory Halls at 3.5 GHz and 28 GHz for Various Antenna Configurations," 3rd Generation Partnership Project, Proposal R1-1906662, May 2019. [Online]. Available: https://www.3gpp.org/ftp/tsg_ran/WG1_RL1/TSGR1_97/Docs/

[68] ZTE, Sanechips, BJTU, and Tongji University, "Pathloss Model in IIoT Scenario," 3rd Generation Partnership Project, Proposal R1-1904227, Apr. 2019. [Online]. Available: https://www.3gpp.org/ftp/tsg_ran/WG1_RL1/TSGR1_96b/Docs/

[69] CMCC, BUPT, and ZTE, "New Measurements and Modelling on 28 GHz Path Loss and LOS Probability in IIoT Scenarios," 3rd Generation Partnership Project, Proposal R1-1908878, Aug. 2019. [Online]. Available: https://www.3gpp.org/ftp/tsg_ran/WG1_RL1/TSGR1_98/Docs/

[70] CEA-LETI, "Channel Characterization in Industrial Environment with High Clutter Density," 3rd Generation Partnership Project, Proposal R1-1904114, Apr. 2019. [Online]. Available: https://www.3gpp.org/ftp/tsg_ran/WG1_RL1/TSGR1_96b/Docs/

[71] Huawei and HiSilicon, "Other Aspects for Channel Modeling for IIoT," 3rd Generation Partnership Project, Proposal R1-1909318, Aug. 2019. [Online]. Available: https://www.3gpp.org/ftp/tsg_ran/WG1_RL1/TSGR1_98/Docs/

[72] NTT DOCOMO, "On Accuracy of InH Path Loss Model of 38.901 for Factory Scenario," 3rd Generation Partnership Project, Proposal R1-1813337, Nov. 2018. [Online]. Available: https://www.3gpp.org/ftp/tsg_ran/WG1_RL1/TSGR1_95/Docs/

[73] Ericsson, "Channel Model for Factory Automation Scenario," 3rd Generation Partnership Project, Proposal R1-1812164, Nov. 2018. [Online]. Available: https://www.3gpp.org/ftp/tsg_ran/WG1_RL1/TSGR1_95/Docs/

[74] Huawei and HiSilicon, "Consideration on Channel Model for Industrial Factory Environment," 3rd Generation Partnership Project, Proposal R1-1812683, Nov. 2018. [Online]. Available: https://www.3gpp.org/ftp/tsg_ran/WG1_RL1/TSGR1_95/Docs/

[75] ZTE, Sanechips, BJTU, and Tongji University, "About IIoT Scenario," 3rd Generation Partnership Project, Proposal R1-1902112, Feb. 2019. [Online]. Available: https://www.3gpp.org/ftp/tsg_ran/WG1_RL1/TSGR1_96/Docs/

[76] Qualcomm Incorporated, "Indoor Industrial Channel Model," 3rd Generation Partnership Project, Proposal R1-1903023, Feb. 2019. [Online]. Available: https://www.3gpp.org/ftp/tsg_ran/WG1_RL1/TSGR1_96/Docs/

[77] Ericsson, "Further Discussion on Channel Modelling for the Indoor Industrial Scenario," 3rd Generation Partnership Project, Proposal R1-1903122, May 2019. [Online]. Available: https://www.3gpp.org/ftp/tsg_ran/WG1_RL1/TSGR1_96/Docs/

[78] ZTE, Sanechips, BJTU, and Tongji University, "LOS Probability Model in IIoT Scenario," 3rd Generation Partnership Project, Proposal R1-1902117, Feb. 2019. [Online]. Available: https://www.3gpp.org/ftp/tsg_ran/WG1_RL1/TSGR1_96/Docs/

[79] Nokia and Nokia Shanghai Bell, "Modeling of Clutter Densities and Antenna Configurations in Industrial Scenarios," 3rd Generation Partnership Project, Proposal R1-1904824, Apr. 2019. [Online]. Available: https://www.3gpp.org/ftp/tsg_ran/WG1_RL1/TSGR1_96b/Docs/

[80] ZTE, Sanechips, BJTU, and Tongji University, "Discussion on LOS Probability Model in IIoT Scenario," 3rd Generation Partnership Project, Proposal R1-1904804, Apr. 2019. [Online]. Available: https://www.3gpp.org/ftp/tsg_ran/WG1_RL1/TSGR1_96bis/Docs/

[81] Ericsson, "Views on the Path Loss and LOS Probability," 3rd Generation Partnership Project, Proposal R1-1907703, May 2019. [Online]. Available: https://www.3gpp.org/ftp/tsg_ran/WG1_RL1/TSGR1_97/Docs/

[82] ZTE and Sanechips, "LOS Probability Model in IIoT Scenario," 3rd Generation Partnership Project, Proposal R1-1908310, Aug. 2019. [Online]. Available: https://www.3gpp.org/ftp/tsg_ran/WG1_RL1/TSGR1_98/Docs/

[83] Z. Irahhauten, G. J. M. Janssen, H. Nikookar, A. Yarovoy, and L. P. Ligthart, "UWB Channel Measurements and Results for Office and Industrial Environments," in *2006 IEEE International Conference on Ultra-Wideband*, Sep. 2006, pp. 225–230.

[84] X. Raimundo, S. Salous, and A. Cheema, "Indoor Dual Polarised Radio Channel Characterisation in the 54 and 70 GHz Bands," *IET Microwaves, Antennas Propagation*, vol. 12, no. 8, pp. 1287–1292, Jun. 2018.

[85] NTT DOCOMO, "Discussion on Delay Spread for Factory Scenario," 3rd Generation Partnership Project, Proposal R1-1902817, Feb. 2019. [Online]. Available: https://www.3gpp.org/ftp/tsg_ran/WG1_RL1/TSGR1_96/Docs/

[86] Huawei and HiSilicon, "Preliminary Channel Measurement on Fast Fading Parameters for Indoor Factory Environment," 3rd Generation Partnership Project, Proposal R1-1904707, Apr. 2019. [Online]. Available: https://www.3gpp.org/ftp/tsg_ran/WG1_RL1/TSGR1_96bis/Docs/

[87] CMCC and BUPT, "New Measurements and Modelling on Fast Fading in IIoT Scenarios," 3rd Generation Partnership Project, Proposal R1-1904743, Nov. 2018. [Online]. Available: https://www.3gpp.org/ftp/tsg_ran/WG1_RL1/TSGR1_96b/Docs/

[88] ZTE, BJTU, and Sanechips, "RMS Delay Spread Model in IIoT Scenario," 3rd Generation Partnership Project, Proposal R1-1906492, May 2019. [Online]. Available: https://www.3gpp.org/ftp/tsg_ran/WG1_RL1/TSGR1_97/Docs/

[89] B. Holfeld, D. Wieruch, L. Raschkowski, T. Wirth, C. Pallasch, W. Herfs, and C. Brecher, "Radio Channel Characterization at 5.85 GHz for Wireless M2M Communication of Industrial Robots," in *2016 IEEE Wireless Communications and Networking Conference*, Apr. 2016, pp. 1–7.

[90] Z. Zhong, Y. Pan, and J. Zhao, "Massive MIMO Channel Measurement and Characterization for Manufacturing Scenario," in *2020 14th European Conference on Antennas and Propagation (EuCAP)*, Mar. 2020, pp. 1–5.

[91] P. Stenumgaard, J. Chilo, J. Ferrer-Coll, and P. Angskog, "Challenges and Conditions for Wireless Machine-to-Machine Communications in Industrial Environments," *IEEE Communications Magazine*, vol. 51, no. 6, pp. 187–192, Jun. 2013.

[92] NTT DOCOMO, "Discussion on Fast Fading Model for Indoor Industrial Scenarios," 3rd Generation Partnership Project, Proposal

R1-1906232, May 2019. [Online]. Available: https://www.3gpp.org/ftp/tsg_ran/WG1_RL1/TSGR1_97/Docs/

[93] Nokia and Nokia Shanghai Bell, "Delay Spread Measurement Results and Observations from Two Operational Factory Halls at 3.5 GHz for Various Antenna Configurations," 3rd Generation Partnership Project, Proposal R1-1902624, Feb. 2019. [Online]. Available: https://www.3gpp.org/ftp/tsg_ran/WG1_RL1/TSGR1_96/Docs/

[94] E. Tanghe, D. P. Gaillot, M. Liénard, L. Martens, and W. Joseph, "Experimental Analysis of Dense Multipath Components in an Industrial Environment," *IEEE Transactions on Antennas and Propagation*, vol. 62, no. 7, pp. 3797–3805, Jul. 2014.

[95] J. B. Andersen, J. O. Nielsen, G. F. Pedersen, G. Bauch, and J. M. Herdin, "Room Electromagnetics," *IEEE Antennas and Propagation Magazine*, vol. 49, no. 2, pp. 27–33, Apr. 2007.

[96] Ericsson, "Summary of Email Discussion on Fast Fading Modelling and Parameters," 3rd Generation Partnership Project, Proposal R1-1905196, Apr. 2019. [Online]. Available: https://www.3gpp.org/ftp/tsg_ran/WG1_RL1/TSGR1_96b/Docs/

[97] Ericsson and CEA-LETI, "A Review on Delay Spread Results in Industrial Environment," 3rd Generation Partnership Project, Proposal R1-1905202, Apr. 2019. [Online]. Available: https://www.3gpp.org/ftp/tsg_ran/WG1_RL1/TSGR1_96b/Docs/

[98] Ericsson, "Views on the Fast Fading Model and Parameters," 3rd Generation Partnership Project, Proposal R1-1907412, May 2019. [Online]. Available: https://www.3gpp.org/ftp/tsg_ran/WG1_RL1/TSGR1_97/Docs/

[99] Ericsson, "Summary of Email Discussion on Fast Fading Modeling [96b-NR-08e]," 3rd Generation Partnership Project, Proposal R1-1907407, May 2019. [Online]. Available: https://www.3gpp.org/ftp/tsg_ran/WG1_RL1/TSGR1_97/Docs/

[100] Huawei and HiSilicon, "Fast Fading Model for Industrial Factory Environment," 3rd Generation Partnership Project, Proposal R1-1908073, Aug. 2019. [Online]. Available: https://www.3gpp.org/ftp/tsg_ran/WG1_RL1/TSGR1_98/Docs/

[101] Huawei and HiSilicon, "Discussion on Fast Fading Model for Industrial Factory Environment," 3rd Generation Partnership Project, Proposal R1-1906618, May 2019. [Online]. Available: https://www.3gpp.org/ftp/tsg_ran/WG1_RL1/TSGR1_97/Docs/

[102] D. Hampicke, A. Richter, A. Schneider, G. Sommerkorn, R. S. Thoma, and U. Trautwein, "Characterization of the Directional Mobile Radio Channel in Industrial Scenarios, Based on Wideband Propagation Measurements," in *Gateway to 21st Century Communications Village. VTC 1999-Fall. IEEE VTS 50th Vehicular Technology Conference (Cat. No.99CH36324)*, vol. 4, Sep. 1999, pp. 2258–2262 vol.4.

[103] D. Solomitckii, M. Allén, D. Yolchyan, H. Hovsepyan, M. Valkama, and Y. Koucheryavy, "Millimeter-wave Channel Measurements at 28 GHz in Digital Fabrication Facilities," in *2019 16th International Symposium on Wireless Communication Systems (ISWCS)*, Aug. 2019, pp. 548–552.

[104] NTT DOCOMO and Fraunhofer HHI, "Discussion on Fast Fading Model for Indoor Industrial Scenarios," 3rd Generation Partnership Project, Proposal R1-1904971, Apr. 2018. [Online]. Available: https://www.3gpp.org/ftp/tsg_ran/WG1_RL1/TSGR1_96b/Docs/

[105] Ericsson, "Views on Additional Modelling Components," 3rd Generation Partnership Project, Proposal R1-1905203, Apr. 2019. [Online]. Available: https://www.3gpp.org/ftp/tsg_ran/WG1_RL1/TSGR1_96b/Docs/

[106] 3GPP, "Study on Evaluation Methodology of New Vehicle-to-Everything (V2X) use cases for LTE and NR;," 3rd Generation Partnership Project, Technical Report TR 37.885, Jun. 2019, v15.3.0. [Online]. Available: https://www.3gpp.org/ftp/Specs/archive/37_series/37.885/

[107] Ericsson, "Summary of Email Discussion on Additional Modeling Components [96b-NR-08f]," 3rd Generation Partnership Project, Proposal R1-1907408, May 2019. [Online]. Available: https://www.3gpp.org/ftp/tsg_ran/WG1_RL1/TSGR1_97/Docs/

[108] Ericsson, "Views on Additional Modeling Components," 3rd Generation Partnership Project, Proposal R1-1907413, May 2019. [Online]. Available: https://www.3gpp.org/ftp/tsg_ran/WG1_RL1/TSGR1_97/Docs/

[109] ZTE, Sanechips, BJTU, and Tongji University, "Absolute Time of Arrival Model in IIoT Scenario," 3rd Generation Partnership Project, Proposal R1-1904118, Apr. 2019. [Online]. Available: https://www.3gpp.org/ftp/tsg_ran/WG1_RL1/TSGR1_96b/Docs/

[110] ZTE, Sanechips, and BJTU, "About Absolute Time of Arrival Model in IIoT Scenario," 3rd Generation Partnership Project, Proposal R1-1906493, May 2019. [Online]. Available: https://www.3gpp.org/ftp/tsg_ran/WG1_RL1/TSGR1_97/Docs/

[111] NTT DOCOMO, "Proposal for Additional Delay for Absolute Time Arrival Modeling in NLOS Environment," 3rd Generation Partnership Project, Proposal R1-1904972, Apr. 2018. [Online]. Available: https://www.3gpp.org/ftp/tsg_ran/WG1_RL1/TSGR1_96b/Docs/

[112] NTT DOCOMO, "Proposal for Additional Delay for Absolute Time Arrival Modeling in NLOS Environment," 3rd Generation Partnership Project, Proposal R1-1906233, May 2019. [Online]. Available: https://www.3gpp.org/ftp/tsg_ran/WG1_RL1/TSGR1_97/Docs/

[113] Ericsson, "Summary of Email Discussion on Additional Modelling Components," 3rd Generation Partnership Project, Proposal R1-1905197, Apr. 2019. [Online]. Available: https://www.3gpp.org/ftp/tsg_ran/WG1_RL1/TSGR1_96b/Docs/

[114] Huawei and HiSilicon, "Modelling of Absolute Delay for Positioning in Industrial IoT Environments," 3rd Generation Partnership Project, Proposal R1-1905734, Apr. 2019. [Online]. Available: https://www.3gpp.org/ftp/tsg_ran/WG1_RL1/TSGR1_96b/Docs/

[115] Huawei and HiSilicon, "Modelling of Absolute Delay for Positioning in Industrial IoT Environments," 3rd Generation Partnership Project, Proposal R1-1906622, May 2019. [Online]. Available: https://www.3gpp.org/ftp/tsg_ran/WG1_RL1/TSGR1_97/Docs/

[116] ZTE and Sanechips, "Additional Modeling Components to Support IIoT," 3rd Generation Partnership Project, Proposal R1-1908314, Aug. 2019. [Online]. Available: https://www.3gpp.org/ftp/tsg_ran/WG1_RL1/TSGR1_98/Docs/

[117] Ericsson, "Absolute Delay Modeling," 3rd Generation Partnership Project, Proposal R1-1909336, Aug. 2019. [Online]. Available: https://www.3gpp.org/ftp/tsg_ran/WG1_RL1/TSGR1_98/Docs/

Tao Jiang Received the B.S. degree in communication engineering from the Huazhong University of Science and Technology, Wuhan, China, in 2015 and completed two years of M.S. courses in the Beijing University of Posts and Telecommunications School of Information and Communication Engineering, Beijing, China in 2017, where he is currently working toward the Ph.D. degree in information and communication engineering. His current research interests include mmWave, IoT, V2V channel modelling.

Jianhua Zhang Received B.S. from the North China University of Technology in 1994 and Ph.D. degrees from the Beijing University of Posts and Telecommunications (BUPT) in 2003. Now she is the professor of information and engineering college, BUPT. She has published more than 70 journal papers and nearly 200 conference papers. She received China Communications Best Paper award at 2016 and shared VTC 2015 spring, JCN2009 best paper awards. She continuously contributed to channel model standards from ITU-R M.2135 to 3GPP 36.873,900/901 and she was the Drafting Group (DG) Chairwoman of ITU-R IMT-2020 channel model. Her research interests are massive MIMO and millimeter wave channel modelling and transmission techniques, channel emulator, OTA test and etc.

Pan Tang Received the B.S. degree in electrical information engineering from the South China University of Technology, Guangzhou, China, in 2013 and completed two years of M.S. courses in the Beijing University of Posts and Telecommunications School of Information and Communication Engineering, Beijing, China in 2015, where he is currently working toward the Ph.D. degree in information and communication engineering. From 2017 to 2018, he was a Visiting Scholar with the University of Southern California. His current research interests include mmWave channel modeling, V2V channel modeling and signal estimation.

Lei Tian Received the B.S. degree in Communication Engineering and Ph.D. degree in Information and Communication Systems from Beijing University of Posts and Telecommunications (BUPT) in 2009 and 2015, respectively. He has been dedicated to the research on wireless channel measurement and modeling, including wireless wideband channel measurement method, MIMO channel measurement method, channel parameter estimation, modeling of large-scale and small-scale channel characteristics, and wireless channel modeling.

Yi Zheng Received the B.S. and M.S. degrees from the Beijing University of Posts and Telecommunications in 2007 and 2010, respectively. He is currently with the China Mobile Research Institute as a standard engineer engaging in 3GPP and ITU. His research interests include MIMO, millimeter wave, channel measurement and modeling.

Jianwu Dou Received the Ph.D. degree in robotic mechanism from the Beijing University of Technology, Beijing, China, in 2001.,From 2000 to 2014, he was the Head of Wireless RRM Team, including 2G/3G/4G/WLAN and was in charge of developing a multi-RAT wireless system simulation platform. From 2012 to 2014, he was the Chief engineer and Product Manager of ZTE iNES. From 2005 to 2017, he was the Vice Director of the Wireless Algorithm Department, ZTE Corporation, Shenzhen, China. He was in charge of the National Major Project and participated in two 5G projects supported by the Ministry of Industry and Information Technology of China. From 2014 to 2020, he participated the standard work in 5G channel modeling/UAV/NTN/IIOT channel modeling in 3GPP and IMT2020 channel modeling in ITU-R. His current research interests include B5G/6G channel modeling, meta-material, THz, unmanned aerial vehicle and satellite communication., Dr. Dou was a recipient of the Science and Technology Award (1st Level) from the China Institute of Communications from 2014 to 2015, the Award for Chinese Outstanding Patented Invention from WIPO-SIPO in 2011, and Shanghai science and technology award in 2015.

Henrik Asplund Received the M.Sc. degree in Engineering Physics from Uppsala University, Sweden, in 1996. He joined Ericsson in 1996 where his research on propagation and channel modeling has contributed to the standardization, product development and deployment of wireless systems from 2G to 5G. He has represented Ericsson on topics related to propagation in ITU-R WP5D and 3GPP RAN1 and has served as the rapporteur for the 3GPP study item on Channel modeling for indoor industrial scenarios. Currently, he holds a position as master researcher at Ericsson Research, Ericsson AB, Sweden, where his research areas of interest include propagation measurements and modeling for 5G as well as beamforming and multi-antenna communications.

Leszek Raschkowski Received the Dipl.-Ing. (M.S.) degree in Electrical Engineering from Technische Universität Berlin, Germany in 2012. Currently, he is employed as a research associate and project manager at Fraunhofer Heinrich Hertz Institute in Berlin, Germany. Leszek is working on several research projects in the field of wireless communications. In addition, he is actively contributing to 3GPP standardization work related to the radio access network as a regular delegate since 2013. At the moment, he works on the integration of non-terrestrial networks (satellite constellations) into the 5G ecosystem. His research interests include measuring, modeling and simulating radio propagation channels, as well as performance analysis of wireless communication systems. This encompasses 3D MIMO, deployments in industrial factory halls, aerial vehicles (drones) and satellites.

Raffaele D'Errico Received the Laurea degree (summa cum laude) in Telecommunications Engineering from the University of Bologna, Italy, in 2005, and the PhD degree in Physics from University of Orsay (Paris, France) and in Electronics, Information and Telecommunication Engineering from University of Bologna. Since 2008 he's with CEA-LETI Grenoble France, as senior scientist and project manager. He participated to COST actions 2100 and IC1004, were he served as chair of the Working Group on "Body Environment", and recently as French Delegate member of the IRACON action on 5G and beyond communications. He authored or coauthored three Best Paper Awards (IEEE PIMRC 2009, IFIP NTMS 2011, and LAPC 2012 Best Student Paper). His research interests concern radio channel sounding and modeling, antenna design and characterization, mmWave technologies, Body Area Networks (BANs), UWB and UHF RFID, localization, cooperative communication protocols, OTA tests, Radar.

Tommi Jämsä Received the M.S. degree in electrical engineering from Oulu University in 1995. He joined Elektrobit (EB) in 1993. Since then, his responsibilities have been product management, radio channel research, product development, and standardization of channel models and test methodologies. Since 2006, he has contributed channel models and test methodologies to several international forums such as COST, WiMAX Forum, 3GPP, and ITU-R. He acted as a work package leader in IST-WINNER project and chaired channel modeling group in ITU-R WP5D. In 2013, he started as a Senior Manager in Research and Technology at Anite Telecoms where he was leading 5G channel modeling activities in the European METIS project until early 2015. He established a private company, Tommi Jamsa Consulting, in January 2015, and worked for Huawei Technologies in Sweden, where his responsibilities were standardization, 5G channel models and OTA test methods. In January 2020, he was nominated as a Senior Expert, Intelligent Automotive Solutions, at Huawei Munich Research Center.